DESIGNING SILICON BASED ANODE FOR

LITHIUM-ION BATTERIES

By

TIANXIANG NING

Bachelor of Engineering in

Materials Science and Engineering

Hunan University

Changsha, Hunan

2014

DESIGNING SILICON BASED ANODE FOR

LITHIUM-ION BATTERIES

Thesis Approved:

Dr. Raj N. Singh

Thesis Adviser

Dr. Krishnan Ranji Vaidyanathan

Dr. Nirmal Govindaraju

ACKNOWLEDGEMENTS

I would like to express my sincere appreciation to my advisor, Dr. Raj Singh, for giving me the chance to work on this project and accepting me into his research group, for his guidance, financial assistance and constant encouragement throughout my study. I would also like to thank Dr. Malay Jana for his guidance and assistance through all the iterations of this research. I appreciate all my research group members for their support and guidance during my master's life. I also wish to thank Dr. Ranji Vaidyanathan and Dr. Nirmal Govindaraju, for their assistance and service on my thesis committee.

I would also like to thank Oklahoma State University and Materials Science and Engineering department faculty, for their financial and technical assistances. Special thanks to MACCOR Inc. for their battery testing system.

Finally, words cannot express my gratitude for unwavering support of my family. I would like to give my deepest respect and thanks to my father and mother for their love, continued support and understanding during my study to finish my research work.

Name: TIANXIANG NING

Date of Degree: MAY, 2017

Title of Study: DESIGNING SILICON BASED ANODE FOR LITHIUM-ION
BATTERIES

Major Field: MATERIALS SCIENCE AND ENGINEERING

Abstract: Lithium-ion batteries (LIBs) are the most widely used energy storage devices at present, especially in portable electronic devices. However, to satisfy the requirement of electric vehicles and other applications like grid storage, the current commercial graphite based anodes are limited by their theoretical capacity of 372mAh/g. Among a variety of alternative to replace graphite, silicon is a promising anode material because of its high theoretical capacity of 4200mAh/g. However, the capacity of these anodes fade quickly after few initial cycles of operation because of stresses induced by large volume expansion of the silicon during lithiation, which primarily results in fracture of particles. To overcome this issue, several strategies have been employed, for example, reducing the size of silicon and making composite with other materials. But often these methods are difficult to achieve a stable and reversible capacity after many cycles and are not cost effective. In this study, an innovative method is used for realizing a high reversible capacity anode based on silicon by negating the effect of volume expansion, based on low cost metallurgical grade polycrystalline silicon powder. In this approach, first the silicon nanowires are created by metal assisted chemical etching and then a rapid freezing of the solution containing superconductive carbon particles and etched silicon particles in furfuryl alcohol is carried out. In the next step, the mixture is pyrolyzed for getting conformal coating of carbon on the etched silicon particles. The coating together with the highly conducting phase of carbon not only improves the conductivity of the electrode (both the connection between the active particles and with the current collector) but also provides the flexibility for managing the volume expansion during lithiation. The resultant material exhibited a reversible specific capacity of more than 1200mAh/g after 50 cycles with a coulombic efficiency of 99.6%.

TABLE OF CONTENTS

LIST OF TABLES

LIST OF FIGURES

CHAPTER I

INTRODUCTION

1.1 Motivation

To solve the environmental issues such as global warming, air pollution because of relying on fossil fuel, it is desirable to use renewable energy, which requires an effective energy storage device. Batteries are one of the suitable electrical energy storage devices because they have big range of energy density and power density to satisfy different demands, high efficiency and long lifetime [1]. A battery is a device that converts the chemical energy contained in its active materials directly into electric energy by electrochemical oxidation-reduction (redox) reaction. In general, battery can be divided into primary battery (non-rechargeable) or secondary battery (rechargeable) [1]. Among a variety of choices for energy storage devices, Li-ion batteries (LIBs) are well known as a reliable choice because of the good life cycle, high power capacity and low cost. Li-ion batteries are rechargeable, which is comprised of cells that employ lithium intercalation compounds as the positive and negative electrodes.

There are many areas of research in the field of Li-ion battery, such as anode, cathode, electrolytes, binders and even the design of the cell. This study focuses on the development of high capacity anode based on silicon for lithium-ion batteries.

Until now, carbon based materials are regarded as the standard anode for the LIBs. Usually made of graphite, these anodes have a theoretical capacity of 372mAh/g, low operating voltage and good cycle lifetime [2]. However, the low capacity and a low specific energy of ~150Wh/kg are

1

far below specific energy required of more than 200Wh/kg for electric vehicles and new generation portable devices [2]. Alternative anode materials include different kinds of alloying metals, conversion materials, for example silicon, tin, titanium oxide, iron oxide etc. In this context, silicon has been regarded as one of the most promising candidate as an anode material for high energy density LIBs, due to its high theoretic specific capacity (4200mAh/g) [2], which is more than 10 times higher than that of the commercial graphitic carbon anodes. However, the poor cycling performance because of the large volume expansion (can reach to 400%) of silicon during electrochemical reaction has been an impediment to its development [2]. After volume expansion, silicon being a brittle material, cannot withstand the resulting cracks due to the high stresses generated by the volume expansion, causing active material to break into smaller pieces and isolate from the rest of the electrode. In addition, due to the same reason, the interface between the electrode and its current collector (copper foil) can be compromised, causing entire sections of the electrode to loosen. Even though the material is contained inside the battery, both of these effects cause parts of the electrode to lose electrical contact with the rest of the electrode. When the electrical contact is lost, the specific capacity starts decreasing quickly.

To solve this vital problem, researchers have tried many methods. One common method is to minimize the particle size of silicon to minimize the stresses caused by the volume expansion. In this way, many kinds of nanostructures are developed, such as nanowires, nanotubes and thin-films have shown good initial capacity and better cycling performance than the bulk silicon particles. Another approach is to incorporate small size silicon particles into a conductive matrix, creating a composite electrode. The matrix serves in both ways by increasing the conductivity of the electrode and to accommodate the volume expansion of the silicon particles. However, these methods also have problems of high cost and complicated technology.

In this study, low-grade polycrystalline silicon as the major active material has been designed in such a way as to use its high capacity in LIBs. The silicon nanowires (SiNWs) were synthesized through a modified metal-assisted chemical etching of polycrystalline silicon particles, which is

much cheaper than the single-crystalline silicon. Then those SiNWs were coated with carbon in an innovative approach, which further improved the battery life by negating the effect of the volume expansion of silicon.

1.2 Thesis outline

The content of the thesis is presented in six chapters as outlined below:

Chapter 1 is a general introduction of the study and describes the motivation behind this study.

Chapter 2 contains the literature review related to this study. It includes an overview of the rechargeable batteries, especially the lithium-ion batteries, a brief history, basic concepts and the recent research achievements of this field.

Chapter 3 describes the objectives of this research work.

Chapter 4 presents the overall procedures and experiments carried out during this study, and the raw materials and chemicals used in the synthesis and fabrication. The physical and structural characterizations include Scanning Electron Microscopy (SEM), X-ray diffraction (XRD) and Raman spectroscopy, Fourier Transform Infrared Spectroscopy (FTIR). The details of the experimental setup for making the coin cell and different electrochemical characterizations such as Cyclic Voltammetry (CV) and Electrochemical Impedance Spectroscopy (EIS), charge-discharge are also presented in this chapter.

Chapter 5 describes the results and discussion (i) on processing of the electrode starting from fabrication of SiNWs and its coating and (ii) about the electrochemical performances of the resulting electrode.

Chapter 6 provides the major conclusions of this study.

Chapter 7 gives suggestions for future research.

CHAPTER II

REVIEW OF LITERATURE*

2.1 Introduction to secondary batteries

Rechargeable batteries or secondary batteries, are types of batteries, which can be charged and discharged many times in their lifetime, such as, Lead-acid batteries, Nickel-Cadmium batteries and Lithium-ion batteries. They are used in many applications, such as daily consumer electronics (e.g. mobile phones, laptops, tablets etc.) and electric vehicles. The mapping of energy density Vs. specific energy of different kinds of rechargeable batteries shown in Figure. 2.1 justify the emergence of Li-ion battery as the primary option among others [3].

In lithium ion batteries, there are three major components, namely cathode, anode and electrolyte. The cathode material is typically a metal oxide having layered structure, for example lithium cobalt oxide ($LiCoO_2$), mixed with a conductive material, such as carbon black, and binder, typically polyvinylidene fluoride (PVDF) on a current collector of aluminum foil. The anode material is typically a graphitic carbon material having layered structure and also mixed with conductive carbon black and binder on a copper foil current collector. A microporous polyethylene or polypropylene separator film in products that employ a liquid electrolyte electrically isolates the positive and negative electrodes. The electrolyte (liquid) is typically a lithium salt solution in one or more organic solvents, typically carbonates, such as lithium hexafluorophosphate ($LiPF_6$) solution in 1:1 volume ethylene carbonate (EC) and dimethyl carbonate (DMC) mixed solvents. When a battery is cycled (charged and discharged), lithium

ions (Li^+) intercalate/de-intercalate between the cathode (positive electrode) and anode (negative electrode).

Since the first commercialization of lithium ion batteries by SONY in 1991 till now the market has increased very rapidly. According to the report from Transparency Market Research (TMR), the opportunity in the global lithium-ion battery market is poised to rise from US$29.68 billion in 2015 to US$77.42 billion in 2024, showing a fast Compound Annual Growth Rate (CAGR) of 11.6% therein, especially in automotive sector [4]. The lithium ion batteries have rapidly become the commonly used power source in global markets, and battery performance is supposed to improve the demand from different requirements.

The high specific energy (up to 240Whkg^{-1}) and energy density (up to 400WhL^{-1}) of the commercial products make them attractive for different applications [1, 3]. Figure. 2.1 shows the comparison of the different types of rechargeable batteries in terms of energy density and specific energy.
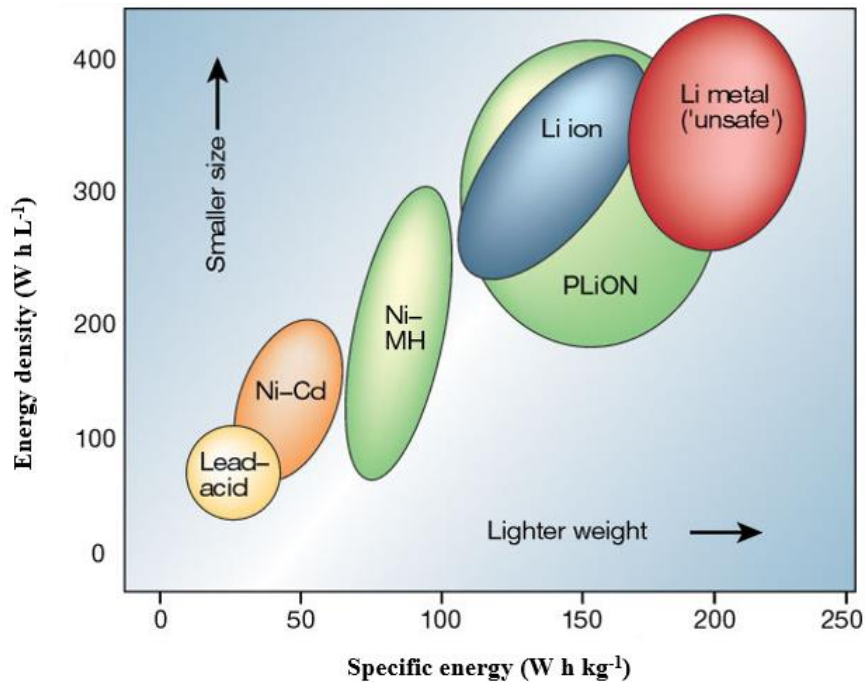
Figure 2.1 Energy density and specific energy of different kinds of rechargeable batteries [3].

The active materials in lithium ion cells run a reversible intercalation process, in which lithium ions are reversibly inserted into or removed from a host electrode without a significant structural change. For example, lithium ion batteries, which are based on alkali metal intercalation of graphite or graphitic carbon. When a lithium ion cell is charged, the active cathode material is oxidized and the active anode material is reduced. The charge-discharge process in a lithium ion cell is illustrated in Fig. 2.2. In this figure, the active materials are shown on metallic current collectors.
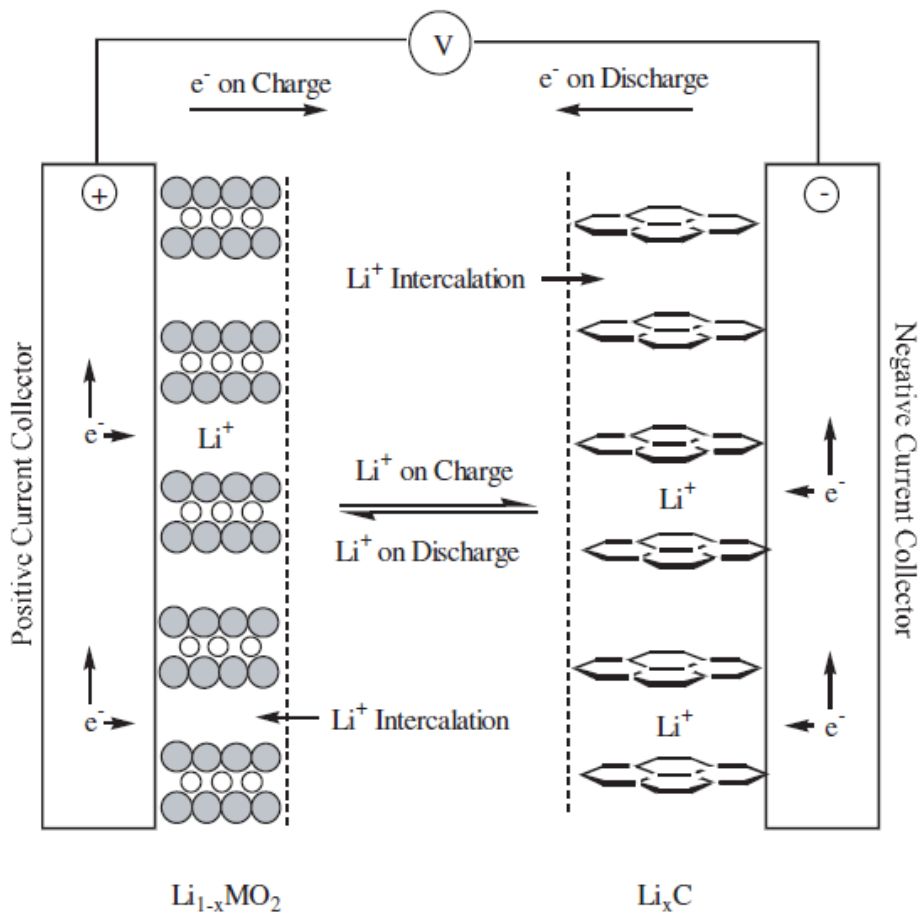
Figure 2.2 Schematic of the electrochemical process in a lithium ion cell [1].

In this process, lithium ions are de-intercalated from the cathode material and intercalated into the anode material, as illustrated in equations (2.1)-(2.2) [1].

6

$$\text{Cathode: LiMO}_2 \underset{\text{disCharge}}{\overset{\text{charge}}{\rightleftarrows}} \text{Li}_{1-x}\text{MO}_2 + x\text{Li}^+ + x\text{e}^- \tag{2.1}$$

$$\text{Anode: C} + x\text{Li}^+ + x\text{e}^- \underset{\text{disCharge}}{\overset{\text{charge}}{\rightleftarrows}} \text{Li}_x\text{C} \tag{2.2}$$
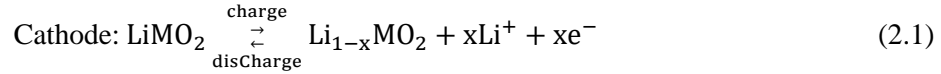
In these equations, $LiMO_2$ represents the metal oxide cathode material, such as $LiCoO_2$, and C is the carbonaceous anode material, such as graphite. x depends on the molar capacities of the active electrode materials for lithium.

Among the three major components in a battery as discussed above, materials for the two electrode materials primarily determines the capacity of the cell/battery. For cathode, there exists three major types of materials such as (i) layered $LiCoO_2$, (ii) spinel type $LiMn_2O_4$ and (iii) olivine $LiFePO_4$ [5]. All these three have their own advantage and disadvantages. In this thesis, our focus is to improve the capacity of the anode half-cell using silicon based anode and hence we will review the state of the art in silicon based anodes-its progress, limitations and challenges with a brief overview of the various type of anode materials.

2.2 Anode materials for lithium ion batteries

Since late 1970s, intercalation electrodes are being considered as one of the contenders for rechargeable lithium ion battery anodes [6]. Initially researchers have focused on lithium metal as anode material, however it has some safety issues such as short circuiting, because lithium metal always deposit as dendrites during the charge and discharge cycles [1]. Since researchers have shown the ability of Li^+ to intercalate/de-intercalate into or from graphite reversibly, it has been used as a reliable anode material for lithium ion batteries [6]. However, the current anode materials are not sufficient to store higher energy required for high capacity batteries. Also, to cope up with the needs of miniaturized device technology there is a need to replace graphite with some high capacity electrode materials. Therefore, research and development on new or improved anode materials has drawn a huge attention by the scientific community. This section will briefly discuss the pros and cons of various kinds of anode materials available or explored for lithium ion batteries.

The Table 2.1 showed the main types of anode materials for lithium ion batteries and their characteristics. As can be seen from Table 2.1 that the active and potential anode materials can be divided into three major groups. First group considers the materials where intercalation/de-intercalation happens through layered structures of the anode such as carbon-based materials. Second group of materials like Si, Ge, Sn via alloying/de-alloying reaction of lithium ions to realize the energy storage. Another group of materials are conversion materials, such as metal oxides, because the conversion reactions with lithium ions during the cycles.

Table 2.1 Categories of common anode materials used for lithium ion batteries [7].

Active anode material	Theoretical capacity (mAh/g)	Advantages	Disadvantages
Insertion/de-insertion materials			
A. Carbonaceous		Good working potential	Low coulombic efficiency
a. Hard carbon	200-600 [8-9]	Low cost	High voltage hysteresis
b. Carbon nanotube (CNT)	1116 [10-12]	Good safety	High irreversible capacity
c. Graphene	780/1116 [13]		
B. Titanium oxides		Extreme safety	Very low capacity
a. $LiTi_4O_5$	175 [14]	Good cycle life	Low energy density
b. TiO_2	330 [14]	Low cost	
		High power capability	
Alloy/de-alloy materials			
a. Silicon	4212 [15]	High specific capacity	High irreversible capacity
b. Germanium	1624 [16-17]	High energy density	Huge capacity fading
c. Tin	993 [18]	Good safety	Poor cycling
d. Antimony	660 [19]		
e. Tin oxide	790 [20]		
f. SiO	1600 [21]		
Conversion materials			
a. Metal oxides (Fe_2O_3, Fe_3O_4, CoO, Mn_xO_y, Cu_2O, NiO, Cr_2O_3, RuO_2, MoO_2 etc.)	500-1200 [17,22-24]	High capacity High energy density Environmental compatibility	Low coulombic efficiency Unstable SEI formation Large potential hysteresis Poor cycle life
b. Metal phosphides / sulfides / nitrides (MXy: M=Fe, Mn, Ni, Cu, Co etc. and X=P,S,N)	500-1800 [24-26]	High capacity Low operation potential and low polarization than counter oxides	Low capacity retention Poor cycle life High cost

2.2.1 Insertion materials

2.2.1.1 Carbon based anode materials

The carbon-based materials are the major anode materials used in commercial lithium ion batteries for more than 25 years due to the abundant availability, thermal stability, low cost, and the ability of lithium intercalation and de-intercalation reversibly [27-30].

The different carbon based materials used as active anodes in lithium ion batteries can be classified into two types depending on the degree of crystallinity and the stacking of carbon atom. One type is called soft carbon (graphitic carbons) in which crystallites are stacked almost in the same direction and the other type is hard carbon (non-graphitic carbons) in which crystallites have disordered orientation. In fact, the former is quite well known in lithium ion batteries, it shows a reversible specific capacity about 350mAh/g and a high coulombic efficiency of more than 90% for more than 100 cycles [8, 27]. Although, graphite is the most commonly used anode material in commercial lithium ion batteries, the low specific capacity limits its application in future next generation batteries [13]. Hence, the use of graphite as anode is still limited to mainly low power devices like cell phones, laptops and cameras. To solve this problem, researchers have tried to use other types of carbon, such as, hard carbon and various nanostructures of carbon.

Hard carbons show high reversible capacity (more than 500mAh/g) in the potential range 0-1.5V Vs. Li/Li$^+$ after 50 cycles [8]. However, the lithium ion diffusion inside hard carbon is very slow, resulting in very poor rate capacity. Other two disadvantages for such materials are low initial coulombic efficiency and low tap density [10-11].

Various nanostructures of carbon e.g. carbon nanotubes (CNTs) are advantageous due to the high surface area accessible for lithium ions to intercalate. The maximum reversible capacity that could be obtained for single walled carbon nanotubes has been estimated to be 1116mAh/g in the first cycle [9-12]. However, it is very hard to achieve such high reversible capacity experimentally. To use CNTs as anode, several attempts were made with a variety of synthesis methods and pre-treatments such as acid treatment, ball milling and surface modifications [11,

31]. Although, at present a popular research direction of CNTs is mixing with other nanostructured materials, which have lower conductivity, such as Si, Ge, or metal oxides, Fe_2O_3, CoO etc., to increase the overall conductivity of the mixture [32]. Even though, CNTs are attractive because of the high capacity but their applications in lithium ion batteries still have issues such as the cost of mass production and the complicated synthesis for such materials for getting the maximum reversible capacity out of it [33].

2.2.1.2 Titanium oxide based anode materials

Among various choices of oxide based materials for lithium battery anodes, lithium titanium oxides (LTO) and titanium oxides (TiO_2) have drawn significant attention in the lithium ion battery field because of their excellent cycling life and low volume change during electrochemical reaction along with low production cost and low risk due to toxicity [14-16, 34-35]. In titanium-based oxides, spinel $Li_4Ti_5O_{12}$ (LTO) is considered the most suitable material for lithium ion batteries because it shows very good lithium ion reversibility at the high operating potential of 1.55V vs. Li/Li^+. Especially, during the insertion process, the spinel LTO symmetry and its structure remain almost unchanged [30, 33, 36]. Hence, LTO has very good cycle life and stability as an anode material in lithium ion batteries. However, this material has two main drawbacks, one is the low theoretical capacity, only 175mAh/g, and the other is the low electronic conductivity only about 10^{-13}S/cm, which restricts the charge and discharge rate [37]. Titanium dioxide (TiO_2) can also be a promising anode material for lithium ion batteries, because it is easy to scale and the cost is not expensive. In addition, titanium dioxide has very good safety and stability at the operating potential of 1.5V vs. Li/Li^+. Moreover, titanium dioxide has excellent high electrochemical activity, strong oxidation capability, and high structural diversity [34, 38]. These characteristics make titanium dioxide a promising candidate as anode material in lithium ion batteries. In fact, 1mol titanium dioxide can host 1mol of lithium with a theoretical capacity of 330mAh/g, which is twice of LTO. However, practical challenge remains in getting the entire capacity. In fact, the process of lithium intercalation and de-intercalation in TiO_2 depends on its

crystallinity, crystal structure, particle size and surface area. Also, because titanium dioxide has many allotropic forms, their electrochemical performance varies accordingly. Among all allotropic forms, rutile form of TiO_2 is most popular studied for anode material in lithium ion batteries. As an example, the rutile form of TiO_2 with particle size of 300nm, has shown the specific capacity of 110mAh/g at first cycle and subsequent stable specific capacity of 50mAh/g over 20 cycles, at the charge/discharge rate 0.1C and when the particle size decreases to 15nm, the initial specific capacity increases to 378mAh/g and after 20 cycles, the specific capacity becomes 200mAh/g. Although titanium based oxides anodes for LIBs show a stable cycle life, but the very low capacity (less than 300mAh/g) restricts their applications, especially when high capacity is the major requirement [16].

2.2.2 Conversion materials

Conversion anode materials refer to transition metal compounds such as oxides, phosphides, and nitrides (M_xN_y: M= Fe, Co, Cu, Mn, Ni and N= O, S, P and N) that are utilized as anode materials in lithium ion batteries.

The electrochemical mechanism of these materials involves their reaction with lithium ions. The electrochemical reactions can be described by equation 2.3 [24, 36].

$$M_xN_y + zLi^+ + ze^- \leftrightarrow Li_zN_y + xM \qquad (2.3)$$
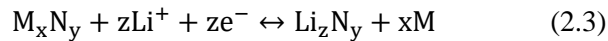
In this equation, M= Fe, Co, Cu, Mn, Ni and N= O, S, P, N.

These materials show high reversible capacities (500-1800mAh/g), and are low cost and non-toxic [22-23]. For example, the hematite form of iron oxide (α-Fe_2O_3) has the theoretical capacity of 1007mAh/g and for magnetite (Fe_3O_4) it is 930mAh/g [39]. Oxides of cobalt (Co_3O_4 and CoO) are other candidates for lithium ion battery anodes. However, they both suffered from poor cycling life because of low electrical conductivity, low diffusion of lithium ions and iron aggregation during charge/discharge process [40]. The respective theoretical capacities of these (Co_3O_4 and CoO) are 890mAh/g and 715mAh/g [41].

Other metal oxides, such as NiO, MnO_x, CuO_x, MoO_x, CrO_x were also studied as anode materials for lithium ion batteries and they revealed miscellaneous physical and chemical properties and a reversible capacity around 500mAh/g [42-46]. Like other anode materials mentioned before, many different forms of oxides have been studied. Porous materials, nanosheets, nanotubes, nanowires and nanotubes of oxides have been synthesized by various methods, such as wet chemical, solid-state and hydrothermal techniques. Most of the oxide materials suffer from low electrical conductivity and low lithium ion diffusion, which hinder their further application.

Apart from metal oxides, metal phosphides (MP_x), metal sulphides (MS_x) and nitrides (MN_x) are also studied as anode materials for lithium ion batteries. These materials can react with lithium in both ways i.e. by conversion reaction or by insertion/de-insertion reaction. For example, copper, cobalt, iron, nickel and tin phosphides follow the conversion mechanism, but other phosphides and most metal sulphides and nitrides follow insertion/de-insertion mechanism. This depends on the nature of the transition metal and stability of chemical bonding [24-26].

Although, conversion materials anodes have high theoretical capacity and high energy density, these materials are still not considered as a good candidate for commercial lithium ion batteries, because of poor capacity retention and large potential hysteresis [22-26].

2.2.3 Alloying materials

Another class of promising anode materials are the alloying materials. These materials have the potential as anode for the next generation lithium ion batteries, which can satisfy higher energy demand, such as electric vehicles or hybrid electric vehicles due to their high-energy density and very high theoretical capacity. Alloying materials refer to elements, which electrochemically alloy and form compound phases with Li, for example, Mg, Ca, Al, Si, Ge, Ga, Sn, Pb, etc. [16-18]. Among all these alloying materials, silicon is the most promising because of two reasons. First, it has the highest possible theoretical capacity available among other alloying materials and second it is the second most abundant material in the earth crust, which makes it even more advantageous in terms of cost. Although in some case, such as single crystalline silicon particles

12

or wafers, the price is still very high. So, we will be discussing about silicon in more detail in this part.

Alloying materials, in general have the potential to fulfil the demand of high capacity anodes for batteries. Actually, their theoretical capacity ranges from 790mAh/g for tin oxide up to 4200mAh/g for silicon. Even though these materials can provide extremely high volumetric and gravimetric capacity, but they usually suffer from poor cycle life as a result of huge volume expansion upon lithiation [47-48]. This expansion causes active electrode materials to fracture, which finally results in isolation from each fractured particle and also from the current collector. All these affect the conductivity of electrode, which is very crucial in determining the performance of the cell. Thus, the major drawbacks of alloying anodes are the poor cycling life and the high irreversible capacity. In order to overcome these issues, several approaches have been used/employed. Among these, a common approach is to reduce the size of the particles from micro to nano scale, because of their increase surface area, which could help in minimizing the stress due to volume expansion.

Tin has attracted a significant interest, having similar properties of silicon except with lower theoretical capacity, higher potential of 0.6V Vs. Li/Li$^+$ and higher electrical conductivity. However, there is a serious shortcoming of tin that particles fracturing, even when the particle sizes are decreased to under 10nm [49]. Other candidates, such as, germanium (Ge), which has a theoretical capacity of 1623mAh/g, is stable and does not break into smaller particles even for larger particles, but is too expensive for most practical applications [16-17]. Considering the cost effect, zinc (Zn), cadmium (Cd), and lead (Pb) based anodes are good candidate for LIBs, but they also suffered from low gravimetric capacity. Aluminum (Al) based anodes also fractured even at nano scale size [50]. Phosphorus (P) and antimony (Sb) also attracted some interest in recent years, because of good theoretical capacity, and ease of processing. For example, Qian et al. used an amorphous phosphorus/carbon nanocomposite as an anode, which showed a capacity around 2000mAh/g [51], whereas Darwiche et al. demonstrated the pure micrometric antimony as

anode material for Na-ion batteries with a capacity ~ 600mAh/g [52]. However, these two materials are not safe, toxic, and have relatively high working potentials. Especially the phosphorus may form phosphine during the chemical reaction, which is very dangerous because it is a colorless, flammable and toxic gas [51, 52].

Among all the alloying materials, silicon is the most attractive anode material because of its extremely high theoretical capacity of 4200mAh/g, the abundant resource in our world, relatively low potential of 0.4V Vs. Li/Li$^+$, low cost of production, chemical stability and non-toxic [2]. Thus, it is easy to understand why silicon is being considered as the most promising anode material for the next generation high capacity lithium ion batteries. Thus, the silicon based anodes will be further described in next section.

2.2.3.1 Silicon based anodes for lithium ion batteries

Among all anode materials, silicon has the highest volumetric capacity (9786mAh/cm^3) and gravimetric capacity (4200mAh/g) [2]. In addition, silicon is eco-friendly, inexpensive and has low working potential, which prevents the safety issues concerning lithium deposition upon cell overcharge. However, a serious issue of fracture because of the huge volume expansion (~400%) during charge process results in poor cycle life and high irreversible capacity as discussed before thereby preventing it commercialization.

The high theoretical capacity (4200mAh/g) of silicon is due to the formation of Li-Si binary compounds corresponding to the formula of ($Li_{22}Si_5$), because one Si atom can alloy with 4.4 Li ions [53]. This $Li_{22}Si_5$ is amorphous and forms when the charging voltage is near 0V. There is another specific binary compound ($Li_{15}Si_4$) that will be discussed later. Many studies have been carried out on understanding the mechanism of lithiation and delithiation of silicon. A brief illustration of the phases that form during lithiation process is shown in Fig. 2.3 [54]. During lithiation, silicon makes alloy containing Li_xSi and experiences a series of phase transformations as shown in Fig. 2.3.
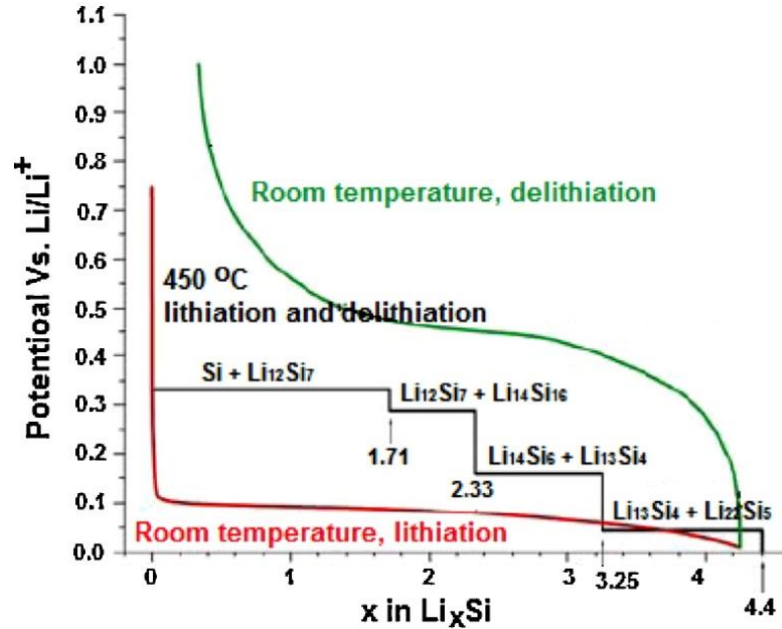
Fig 2.3 Electrochemical lithiation and delithiation curve of silicon at room temperature and high temperature [54].

The black line in Fig. 2.3 indicates theoretical potential curve at high temperature (450°C). Red and green lines represent lithiation and delithiation of crystalline silicon at room temperature, respectively. According to the lithium-silicon phase diagram, when lithium is inserted into silicon, it results in a series of phase transformations, theoretically presented in multiple voltage plateaus in the galvanostatic potential curve (Fig. 2.3, black line) [54]. However, this process only happens at high temperature about 450°C, and when the lithium rich intermetallic phase $Li_{22}Si_5$ formed, the theoretical capacity can reach 4200mAh/g.

Actually, at room temperature, crystalline silicon goes through a crystalline to amorphous phase transformation during the first lithiation and remains amorphous afterwards (Fig. 2.3, green and red line). In some situations, a metastable crystalline $Li_{15}Si_4$ phase has been identified at potentials lower than 0.05V Vs. Li/Li$^+$ at room temperature. The corresponding theoretical capacity of $Li_{15}Si_4$ phase can reach up to 3578mAh/g [53]. The huge volume expansion (300-400%) as a result of transformation of crystalline silicon (c-Si) to either amorphous a-$Li_{22}Si_5$ or

15

crystalline c-Li$_{15}$Si$_4$ can cause cracking and pulverization of the silicon particles, which further results in capacity fading [55-56].

The illustration of fracture of silicon particles is shown in Fig. 2.4.
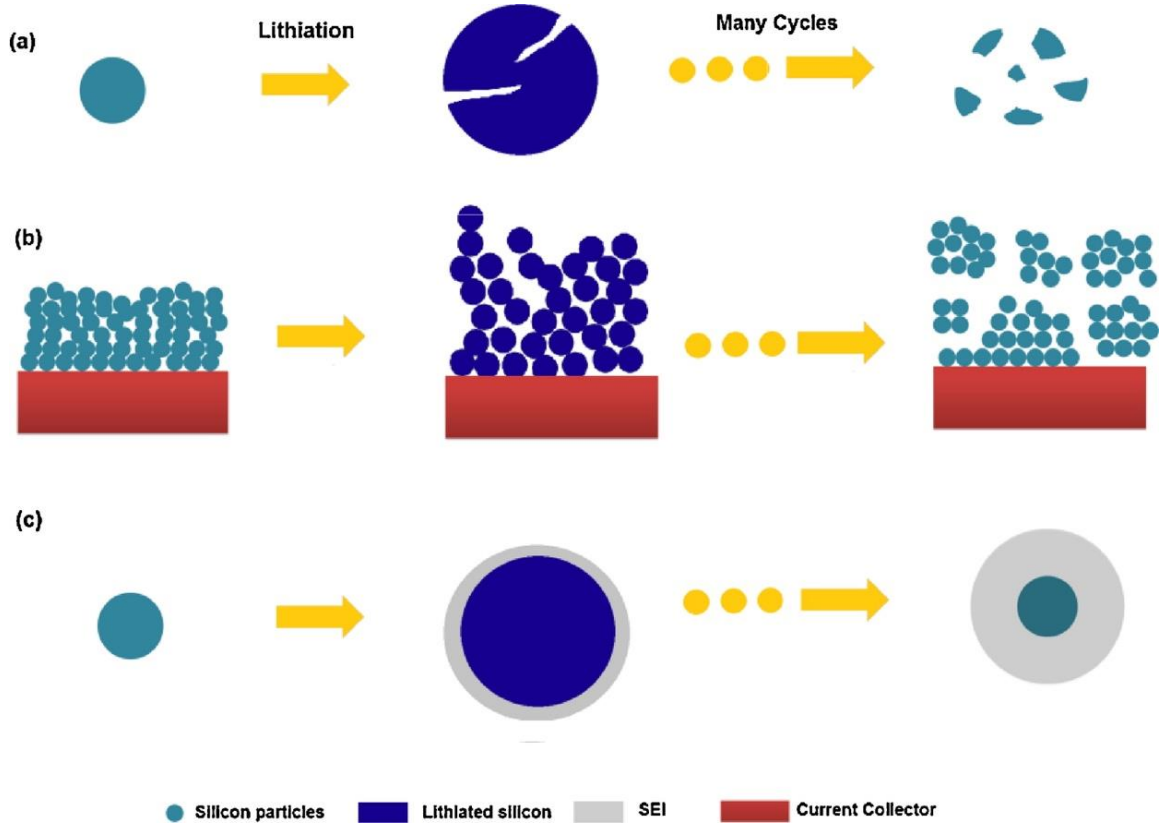
Fig 2.4 Schematics of fracture of silicon particles: (a) Material pulverization. (b) Detachment of fractured particles from each other and current collector as a result of pulverization. (c) Continuous SEI growth [54].

In Fig. 2.4 (a), the silicon particles break into small pieces after several cycles because of the huge volume expansion. As can be seen, after fracture the particle surfaces lose their contacts between them as well as with the current collector (Fig. 2.4 (b)), which prohibits the electrons to flow and hence the capacity starts fading upon cycling. Another important issue of particle fracture is the uncontrolled solid-electrolyte interphase (SEI) formation on the newly exposed surfaces created by the fractured particles on successive cycles (Fig. 2.4 (c)). Solid-electrolyte

interphase (SEI) is a layer on the electrode material surface formed by the decomposition of organic electrolyte at electrode surface when the potential of the anode is below 1V versus Li/Li$^+$. The SEI is ionically conducting and electronically insulating in nature, so it plays a very important role in ionic transport and alloying kinetics. Thus, the SEI needs to be stable and dense during the cycling. But, in fact, as shown in Fig. 2.4 (c), the uncontrolled SEI formation will be a barrier between the electrolyte and the electrode, which will also result the loss of conductivity and capacity fading. All these three issues result in the capacity fading and poor cycle life of silicon based anodes.

Because silicon is a very attractive anode material for lithium ion batteries, a large number of different silicon based electrode designs have been studied to overcome the issue of capacity fading. An overview of these designs will be given in the next section.

2.2.3.1.1 Nanostructured silicon anodes

Nanostructures of silicon in various forms have been used as anodes such as nanotubes, nanowires, hollow spheres, and porous structures [20, 53-65]. These nanostructures have been used by assuming that they can accommodate the huge volume expansion during the lithiation and hence prevent/reduce the stress caused by the expansion. Another assumption is that a nanostructured Si during lithiation can effectively avoid the formation of c-Li$_{15}$Si$_4$, which is detrimental to capacity retention [53-60].

Silicon nanowires as anode for LIBs was reported first time by Cui's group, showing a better electrochemical performance compared to bulk silicon particles [53]. In that work, the SiNWs were prepared through the vapor-liquid-solid synthesis method and directly grown onto stainless steel current collector plate. The schematic structure of SiNWs is illustrated in Fig. 2.5. It can be observed from the figure that the SiNWs array has sufficient empty space to accommodate the huge volume expansion during lithiation. The nanostructures also help in better electron transport through their 1-D structure with nanometric size. The high specific capacity near 4000mAh/g and

capacity retention 75% after 10 cycles at a rate of C/20 was attributed to the structure of the silicon [53].
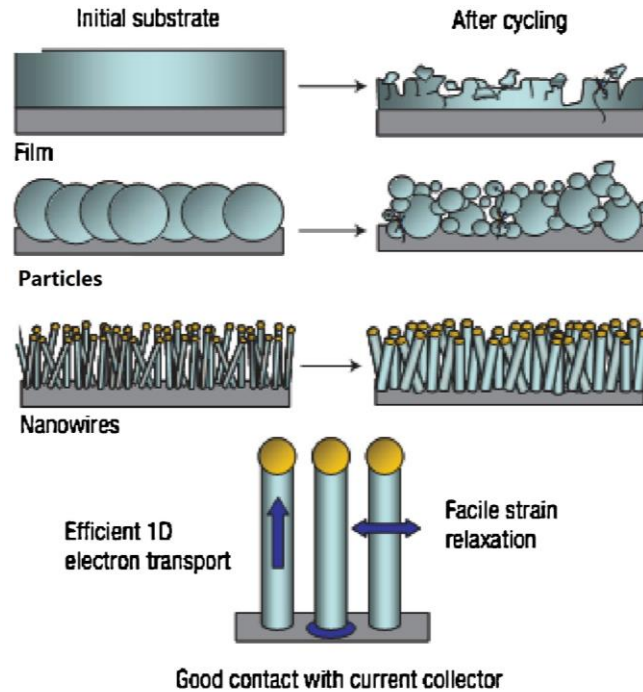
Fig 2.5 Illustration of SiNWs grown on current collector [53].

After the first report of SiNWs anode for LIBs, a large number of related studies have emerged [55-59]. Many different approaches have been used for synthesizing SiNWs. For example, SiNWs were synthesized on stainless steel foil using chemical vapor deposition (CVD) method by Xiao and co-worker. Although the resulting anode revealed a high coulombic efficiency of 89% and a high specific capacity of 2000mAh/g at first cycle, but after 100 cycles the capacity dropped to about 1200mAh/g [57]. Apart from CVD method, metal catalyzed electro-less etching (MCEE) is also used to synthesize SiNWs, as demonstrated by Peng and coworkers [59]. In this case, they fabricated the large-area and wafer-scale arrays of SiNWs by direct electro-less etching of Si wafers [59]. SiNWs synthesized in this way resulted in longer cycle life than bulk silicon [59]. The SiNWs obtained from MCEE showed a discharge capacity of nearly 0.5mAh/cm^2 and longer cycle lifetime. Another, important useful method is metal assisted chemical etching

18

(MACE), which is used in this research work because of its robustness, easy to scale and low cost. In general, MACE is a method using noble metal catalyst (silver, platinum) to enhance the chemical etching on silicon surface [60]. The model of metal assisted chemical etching is that the H_2O_2 oxidant solution will be reduced on the surface of Si, which is covered by noble metal-catalyst, such as silver, holes (h^+) are injected from metal catalyst to Si. Thus, Si, which is underneath of metal catalyst, has highest hole concentration, therefore the chemical etching of Si occurs preferentially underneath the metal. The details of this process will be introduced in the experimental procedure section.

Silicon nanotubes, during lithiation process, can provide buffer space for volume expansion by having increased surface area, which also improves the storage capacity of lithium by providing more contact surface for maximum utilization of the silicon nanotubes [61-62].

Park et al. used silicon nanotubes to increase the surface area accessible to the electrolyte, which allowed Li ions to intercalate at the interior and exterior of the nanotubes [62]. The SEM images of this silicon nanotubes is shown in Fig. 2.6.
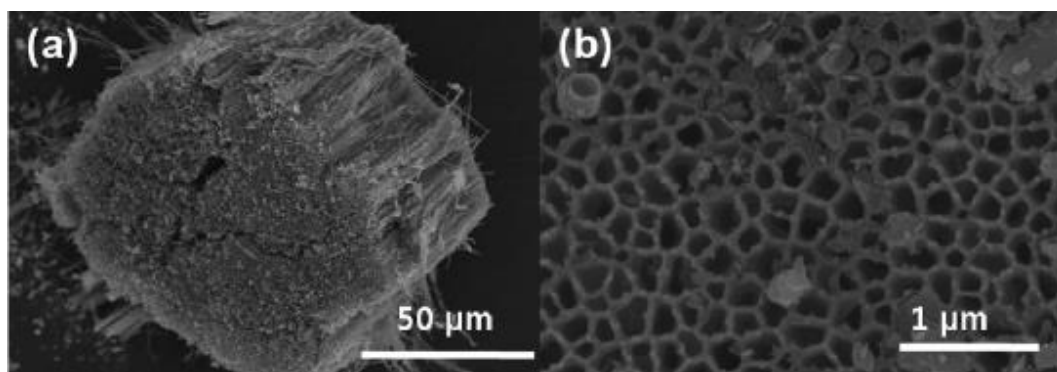
Figure 2.6 SEM images of (a) Side or cross-sectional view and (b) top view of the Si nanotubes [62].

The silicon nanotube anodes reported to have high reversible capacity of 3200mAh/g and capacity retention of 89% after 200 cycles at a constant current rate of 1C [62]. The electrochemical performances are shown in Fig. 2.7.
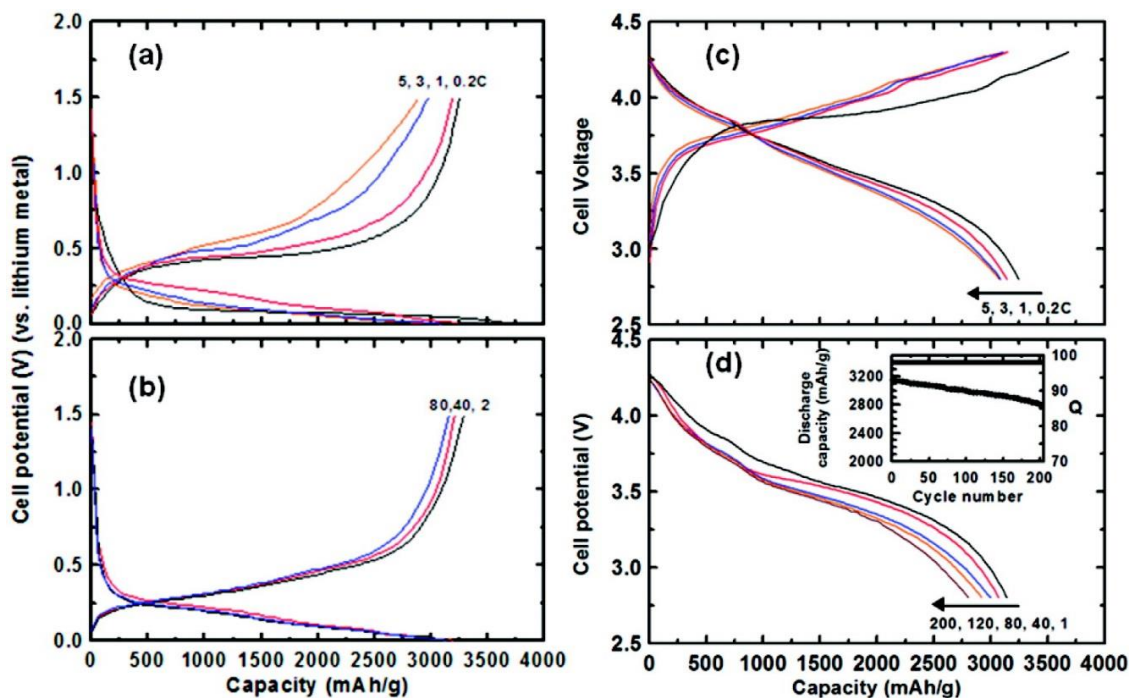
Figure 2.7 (a and b) Rate capability and voltage profiles of the Si nanotubes in coin-type half cells (Vs lithium metal) between 0 and 1.5 V. Cells for (b) were cycled at a rate of 1C between 0 and 1.5 V and voltage profiles were plotted after the 2nd, 40th, and 80th cycles. (c and d) Rate capability and cycle life performance of the Si nanotubes in pouch-type Li-ion cells (cathode was $LiCoO_2$) between 2.75 and 4.3 V to 200 cycles. Rate was increased from 0.2C to 5C with the same rates during charge and discharge. C rate for the cycle test in (d) was 1C [62].

For hollow silicon nanospheres, the working mechanism is almost the same as for the nanotube. During lithiation process, the hollow space provides the buffer region for the thickness of active materials to expand inward without any structural fracture and the structure can be recovered during de-lithiation [63-64].

Hollow silicon nanospheres also shows a better electrochemical performance than the bulk silicon [63-64]. Yao et al. used template method as illustrated in Fig. 2.8, to fabricate the hollow silicon nanospheres [63]. In this method the silica particles (inner R ~175nm) were first coated onto a stainless steel substrate, followed by CVD deposition of Si. The SiO_2 core was then removed by

etching with HF. The SEM and TEM images of the Si nanospheres, synthesized in this way is shown in Fig. 2.9.
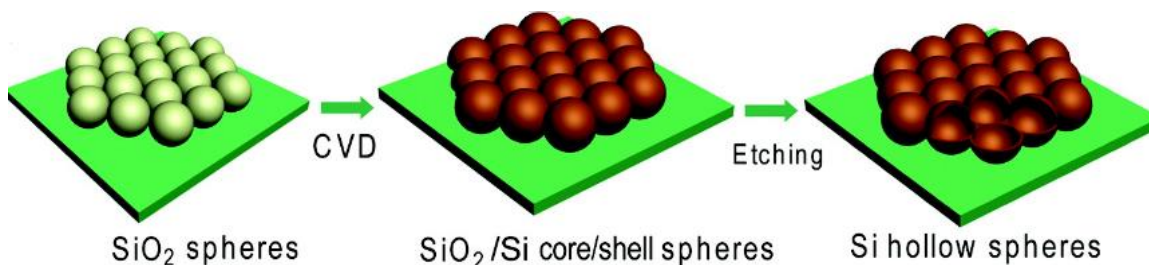
Fig 2.8 Schematic of fabrication of hollow silicon nanospheres on current collector by CVD [63].
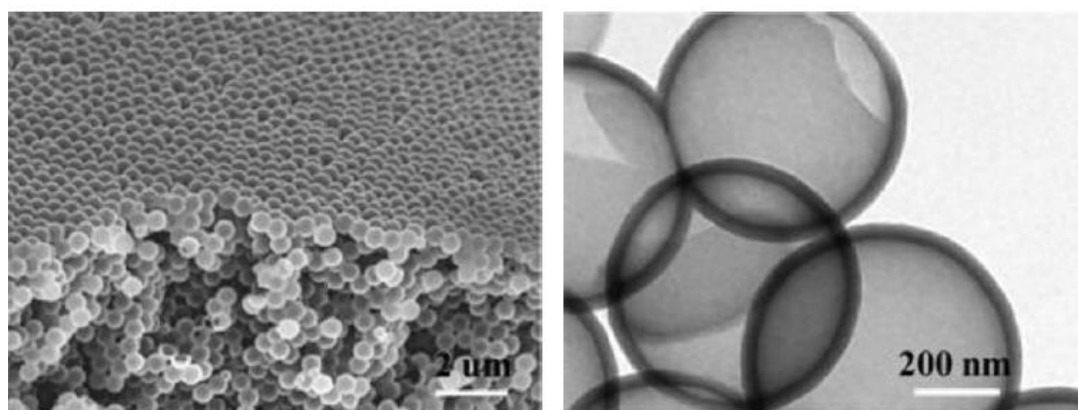
Fig 2.9 SEM and TEM images of Si nanospheres synthesized from silica nanoparticle templates [63].

The anode based on silicon nanosphere grown using silica templates exhibited a high initial discharge specific capacity of 2725mAh/g with a capacity fading of just 8% per 100 cycles at current rate of 1C [63].

Although, a large number of silicon nanostructures have been explored as anodes in lithium ion batteries, but they still have some serious drawbacks such as very high cost of manufacturing and raw materials (especially single crystal silicon powders and single crystal silicon wafers), complicated processing method, which impeded the commercial applications of these materials

[65]. The processing of these anodes also has some additional drawbacks such as they are not easy to scale or cost effective as they mostly employ single crystalline nanostructured silicon and require high precision fabrication technology, which are neither the common practice for Li-ion battery industry nor desirable. Majority of these studies were focused on highly advanced architectures created by means of 3D patterning, electrochemical etching of wafer, template synthesis or by CVD, any of which are not desirable approaches for today's manufacturing practices used for high capacity Li-ion batteries, especially for electric vehicles.

2.2.3.1.2 Silicon based composites

Besides silicon nanostructures, another possible aspect for solving the issue related to the cracking and loose contact is making composites. The composites always used very small fraction of silicon and added with other additive materials (matrix), for example amorphous carbon, graphite, carbon nanofiber, graphene and conductive polymer etc. These materials reveal a very high specific capacity of 1000-3000mAh/g and high capacity retention more than 90% [66-70].

Coating with some conductive materials is also used to eliminate the problem of capacity fading, because after coating, the conductive shell will provide a path for electrons even if the silicon particles are detached with current collector. Carbon coated silicon electrode is a typical silicon/carbon composite. In general, the silicon particles coated with amorphous carbon have shown a specific capacity as high as 1000mAh/g under a current rate of about 0.3mA/mg [66]. Some studies were reported recently, that nano scaled silicon particles in composites improve the capacity retention [67]. Yu and his coworkers demonstrated the electrochemical performances of carbon-coated Si/graphite composites. The composite anode with a ratio of silicon:graphite:carbon equals to 1: 3: 1.53, revealed an initial capacity of 925mAh/g and capacity retention as high as 90% after 40 cycles [67].

Kim et al. used amorphous carbon coated silicon with particle size about 10nm, which revealed a specific capacity of 3000mAh/g with a coulombic efficiency of 98% in the first cycle and have a good capacity retention of 96% after 40 cycles [68]. Besides amorphous carbon, graphene is

another attractive candidate for composite because it improves electron transportation during the charge/discharge process. The synthesis of silicon/graphene composite was achieved using sonochemical method and then magnesiothermic reduction process [69]. In this approach, silica particles were first deposited on the graphene oxide sheets by ultrasonic waves, and then in magnesiothermic reduction process, which utilizes magnesium to reduce the oxidant at low temperature, the silica converts to SiNPs in-situ on graphene sheets. The schematic of the synthesis process of Si/graphene nanocomposite is shown in Fig. 2.10.
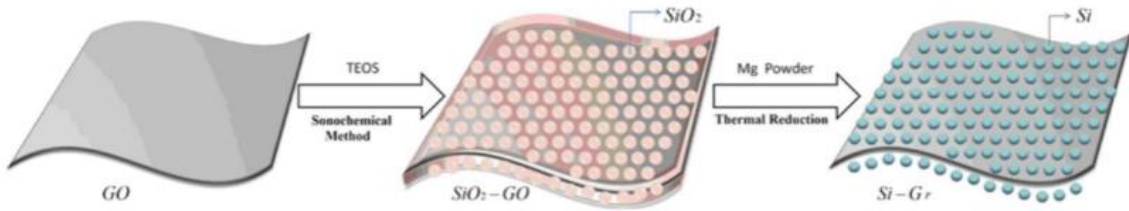
Fig 2.10 Schematic fabrication of Si/graphene nanocomposite [69].

This silicon/graphene composite containing 78wt.% of active material has shown reversible capacity of 1100mAh/g, with very little capacity fading of 9% after 50 cycles [69]. Another example is novel carbon coated silicon nanoparticles (NPs) and reduced graphene oxides (rGO) composites, which were fabricated through layer by layer assembly between carbon coated NPs and graphene oxides nanosheets by filtration. The "sandwich" like structure is shown in Fig. 2.11 [70]. In this example, the Si nanoparticles were first coated by dopamine followed by polymerization and carbonization to get the carbon coated Si nanoparticles, and then coated by reduced graphene oxides on both surface, like a 'sandwich'. This sandwich structure containing carbon coated silicon/graphene oxides composite showed an initial capacity of 1126mAh/g under a current density of 150mA/g, and even after 400cycles, the capacity retention found was 93% [70].

Although, silicon/carbon composite anode could achieve high performances of capacity retention, the key issue of a weak structural interface between carbon and silicon has to be addressed. Also,

their performance especially the capacity depends on the quality of carbon coating and their thickness. Most of the time the coating does not work because of agglomerated particles, which become prominent at nanoscale. They act as a bulk material and upon fracture lose all their contact between individual as well as with the current collector. Thus, coating on individual particles with a robust process is a real challenge. Another serious issue is the high cost of synthesis of silicon/carbon composite, such as CVD or aerosol assisted capillary assembly technique, which rely on a complicated system and high cost of raw materials [69-70].
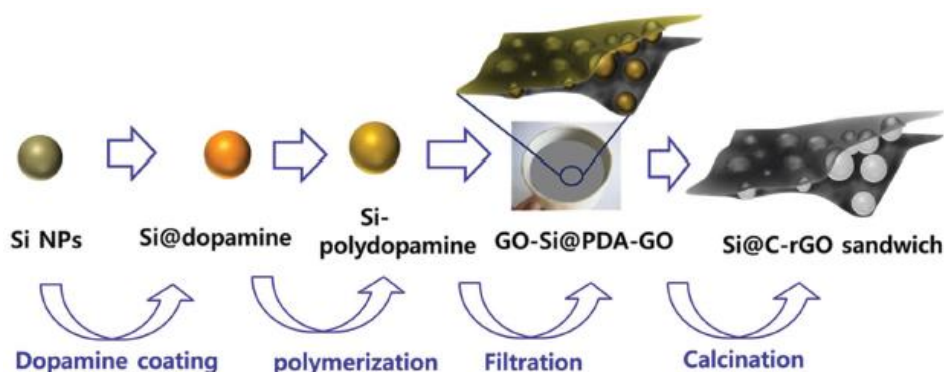
Fig 2.11 Schematic diagram for the synthesis of the carbon coated silicon sandwiched between layers of reduced graphene oxide (rGO) [70].

Besides carbon-based materials, polymer can improve the cyclic performance of the silicon based anode for lithium ion batteries, which can act as a buffer to reduce the impact of the huge volume expansion during the lithiation process. Conducting polymers (CPs) are regularly used in electronics, which reveal many advantages for example good conductivity, flexible mechanical property, and modifiability of the structure. The functions of CPs are not only as a structural and physical buffer to accommodate the mechanical stress, keep the integrity of whole powder based anode and tightly adhere to the current collector (copper foil), but also provide a conductive matrix to improve the conductivity. Among all electronically conducting polymers, polypyrrole (PPy) is the most popular polymer as an electrode additive material in lithium ion batteries because it is easily doped with cations and anions to produce high conductivity and good stability

in air [71-72]. A novel Si/PPy anode using high energy mechanical milling was reported by Guo et al. [71]. This composite anode with a 1:1 weight ratio of Si to PPy exhibited an initial discharge capacity as high as 1800mAh/g with a retention of 90% after 10 cycles. It was claimed that the good performance was due to the buffering and binding ability of the conductive PPy matrix. Another type of composite used is PPy-coated Si nanofibers, which was prepared by using a facile two-step approach: firstly, PPy nanofibers were synthesized by electro-polymerzation and then silicon was deposited on the PPy fibers via a CVD procedure. After this procedure, the PPy nanofibers maintain the electrode integrity and improves the conductivity. The reversible capacity of this composite based anode reported to have specific capacity of about 2800mAh/g with a capacity retention over 91% after 100 cycles [73]. But these conducting polymers are costly and suffer from conductivity and thermal stability, when used at higher temperatures.

Silicon based anodes have huge potential for lithium ion batteries because of the high theoretical capacity, high coulombic efficiency. However, there are still significant challenges that need to be overcome before silicon anodes can be utilized in practical lithium batteries. The challenges include the control and design of silicon based anodes that can either accommodate large volume expansion or structural changes or at least can neglect/nullify the adverse effect of volume change in their properties. Although, in few cases nanoscale morphologies have the potential to achieve long lifetime and good reversible capacity, but the high cost of synthesis is also a serious problem. Using conductive materials, such as carbon or polymer, for building-up a coated silicon anode could provide the long-term stability of the anode and better conductivity. In addition, the flexibility of the exterior shell can provide enough space to allow free expansion of the silicon core while maintaining conductivity between the silicon particles and preventing uncontrolled SEI formation.

* Permissions were obtained for use of all copyright materials in Chapter II.

CHAPTER III

STATEMENT OF OBJECTIVES

The main purpose of this research work is to design a novel silicon based anode material using easily available low grade polycrystalline silicon for lithium ion batteries with high specific reversible capacity.

The motivation for choosing silicon as anode material is its high theoretical capacity of 4200mAh/g [2]. And the main problem of silicon is the stress developed as a result of huge volume expansion during the lithiation, which finally results in fracture of active particles. Considering the various approaches, which the earlier researches have already tried to overcome this issue [55-70], the main objective of this study is to design a robust and effective synthesis process for achieving high performance anode for the lithium ion batteries.

To realize this goal, a low-cost and simple method to fabricate silicon-based anode materials is required. The fabrication process is divided into two parts. The first part is synthesis of silicon nanostructures. In this process, the raw material used for this study is a metallurgical grade polycrystalline silicon powders because of its low cost compared to the single crystalline silicon powders or silicon wafers used in most of the earlier work [53-65]. And for synthesizing the silicon nanostructures, the metal assisted chemical etching (MACE) method is used because of its high efficiency and simplicity. Then a conductive coating of carbon on these etched silicon

particles for providing intercalation path for lithium ions to enter inside silicon is provided. The carbon coating is done using an inexpensive precursor i.e. furfuryl alcohol for the first time to the best of our knowledge for coating silicon based anode materials. Coating on individual particles is a great challenge specially for the application of electrode. Superconducting carbon black as a conductive phase is also used to separate etched silicon particles to avoid agglomeration before coating using furfuryl alcohol solution, which was then pyrolyzed to get a highly conducting carbon coated silicon structures.

Another important objective of the research is to characterize the novel silicon based anode materials for electrochemical performance.

CHAPTER IV

METHODOLOGY

4.1 List of materials

The list of materials and chemicals used for this study to perform various experiments are summarized in table 4.1

Table 4.1 Description of materials and chemicals used in experiments.

Materials/Chemicals	Formula	Purity (%)	Supplier
Polycrystalline Silicon	Si	Metallurgical grade	Globe Metallurgical Inc.
Silver Nitrate	$AgNO_3$	99.9	Sigma-Aldrich
Superconductive Carbon Black powder (SCB)	C	98	US research Nanomaterials, Inc
Hydrofluoric acid	HF	40-45	Sigma-Aldrich
Hydrogen peroxide	H_2O_2	30	Sigma-Aldrich
Nitric acid	HNO_3	65	Sigma-Aldrich
Hydrochloric acid	HCl	38	Fisher chemical
Furfuryl alcohol	$C_5H_6O_2$	98	Acros organics
1-Methyl-2-pyrrolidinone	C_5H_9NO	99.5	Sigma-Aldrich
Polyvinylidene fluoride (PVDF)	$(CH_2CF_2)_n$	-	Sigma-Aldrich
Lithium metal	Li	99.9	Aldrich
Copper foil	Cu	-	MTI
Coin cell (2032type)			MTI
Electrolyte	1.0M $LiPF_6$ in 1:1 EC/DMC (or DEC)		Sigma-Aldrich

4.2 Experimental procedures

4.2.1 Overall framework of the experiments

The overall framework of the experiments for this study is illustrated in Fig. 4.1.
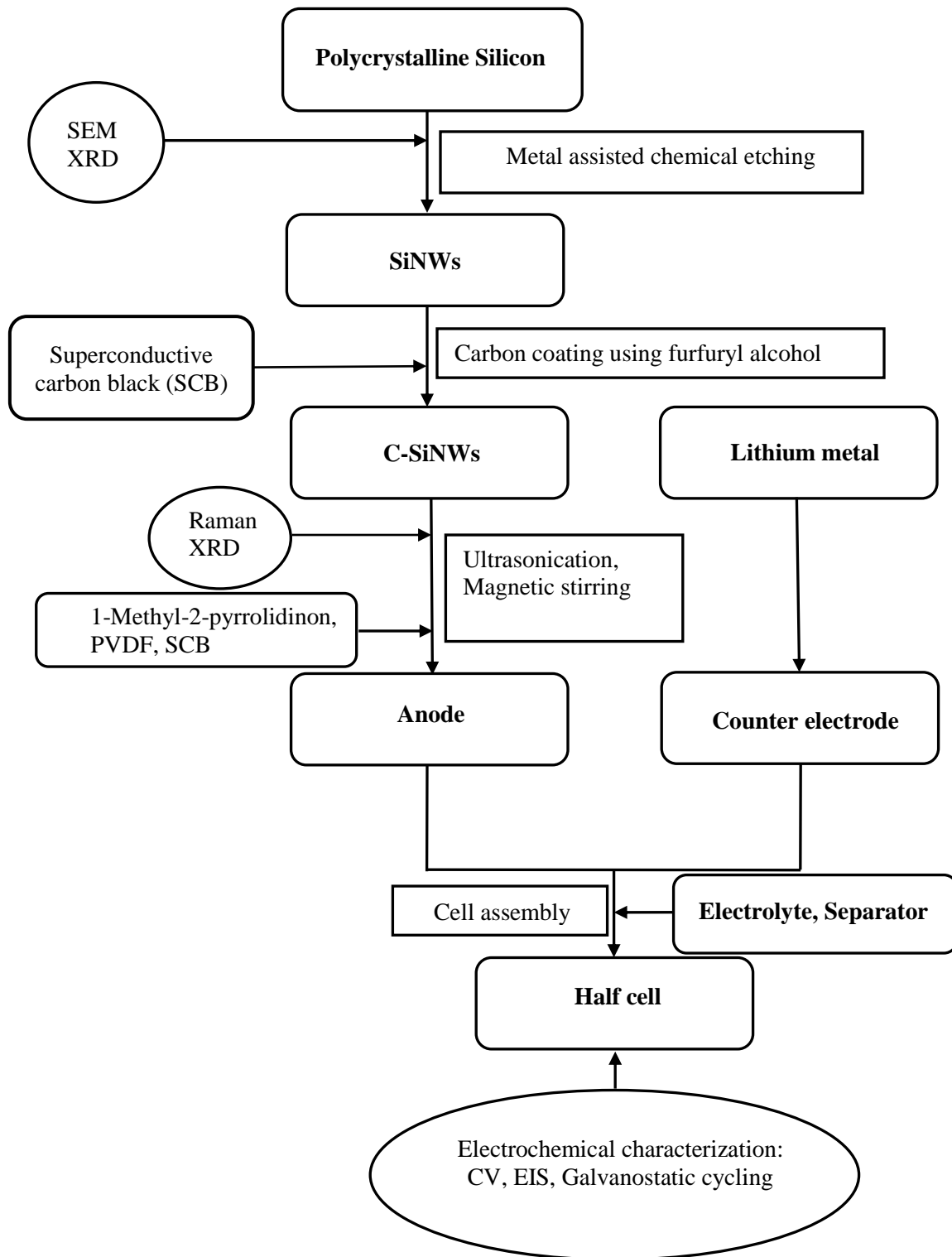
Fig 4.1 The overall framework of the experiments.

4.2.2 Materials synthesis

4.2.2.1 Synthesis of silicon nanowires (SiNWs)

Metal assisted chemical etching was used for the synthesis of silicon nanowires in this research work. At first, micron size polycrystalline Silicon powder (5-100µm; metallurgical grade from Globe Metallurgical Inc.) was cleaned by acetone and 5% concentration of hydrofluoric acid solution to remove native oxide layer and other impurities. After drying, the silicon powder (2.5g in each batch) was uniformly dispersed in etchant solution, containing 0.15g $AgNO_3$ (Sigma Aldrich) in 25ml of 4.6M hydrofluoric acid solution (10ml of 40% HF, Sigma-Aldrich, made to 25ml by mixing with de-ionized water). The mixed solution was put on a magnetic stirrer and while stirring another solution of 0.12M hydrogen peroxide (0.3ml of 30% H_2O_2, Sigma-Aldrich, made to 12.5ml by adding de-ionized water) was added drop wise into the rotating and uniformly premixed solution at an interval of 2-3min for about 30min. The whole mixture was then left for etching the micron size silicon particles at room temperature for 2h to create Si nanowires on the surfaces of the Si particles. The etching process was stopped by adding over 500ml deionized water and the powder was separated by filtering from the solution. Then the filtered powder was added in 30ml nitric acid solution (65%, Sigma-Aldrich) for 20min to remove the silver deposits on the etched particle surfaces and washed thoroughly using deionized water and separated successively using a centrifuge (VWR 13000rpm, 15min). This step was repeated for several times until the pH of the solution became neutral. Finally, the powder was dried before going for the next step of carbon coating. In few cases the silver deposits was reused instead of using new $AgNO_3$.

4.2.2.2 Carbon coating on etched porous silicon with SiNWs

After etching, the etched silicon particles having nanowires were mixed with superconductive carbon black (in powder form) (US Research Nanomaterials, Inc.; size: 5-100nm; conductivity: 2-$4x10^5$S/m; purity: 97.5%) in 90:10 wt. ratio in 20ml acetone to make the solution. It will be shown in next section of results and discussion chapter that how this step of adding a

superconducting phase before carbon coating helps in getting better performance in half-cell. The mixed powders in solution were uniformly mixed by ultrasonicator. And then, after drying, they were added in very small amount of furfuryl alcohol (5-10 ml depending on the volume) (FFA; 98% Acros organic) followed by de-agglomeration and separation of the two phases. After homogeneous and uniform mixing, the solution was suddenly gelled/frozen using few drops of HCl (38% Fisher chemical), which act as an extra polymerizing agent while stirring using a magnetic stirrer. The gelled sample was then dried on hot plate at about 150°C for 2h. The polymer coated sample thus created was kept inside a tubular furnace (Thermolyne Type 59300 High temperature Tube furnace) and the temperature was raised to 600°C and after holding it for 1h, the temperature was further increased to 750°C at a constant heating rate of 5°C/min and held there for 2h under continuous N_2 atmosphere to form a uniform carbon-coating on the etched porous silicon particles, which were networked and separated by the superconductive carbon black. The thickness of the carbon coating was optimized by controlling the amount and concentration of the polymer gel.

4.3 Electrode preparation and coin cell assembly

To fabricate the electrode, the carbon coated porous silicon was ground to fine powder and added with a small amount (2-5wt.%) of superconductive carbon black (97.5%, US Research Nanomaterials, Inc.) and 10wt.% of polyvinylidene fluoride (PVDF) in an N-Methyl pyrrolidine (99.5%, Sigma-Aldrich) solution and mixed to make the slurry. To improve the mixing of slurry, ultrasonicator has been used at least for 1h. After ultrasonication, the slurry was vigorously mixed overnight by using a magnetic stirrer for getting a uniform mixture. Subsequently, the slurry was coated on a single sided polished copper foil (9μm thick 99.99%, MTI Corp.). After drying the organic solvent at 100-120 °C using a hot plate for 10-15min, the coated foil was then transferred to a vacuum oven for storage. The coated foil was pressed using a laminating press to make a relatively dense and uniformly thick electrode. The pressed electrode was cut into small pieces of 1cm^2 to act as an anode for the half-cell. The electrochemical tests were performed in 2032 type

coil cell with the laboratory made by assembling carbon coated etched porous silicon as an active anode material and Li metal (MTI Corp.) as the counter electrode. This cell assembly work was done in an Ar-filled glove-box. The electrolyte used for making the cell contains 1.0 M $LiPF_6$ as lithium salt in 1:1 (w/w) of ethylene carbonate/ diethyl carbonate (Sigma-Aldrich), a mixture of organic solvents. 'Celgard' separator was used for separating the anode from Li (reference electrode) in the coin cells after soaking it in the electrolyte. These separators block the electrical connections between anode and lithium to avoid short circuit but Li ions can move easily through the pores. The half-cell assembly using a 2032 type coin cell is illustrated in Fig. 4.2.
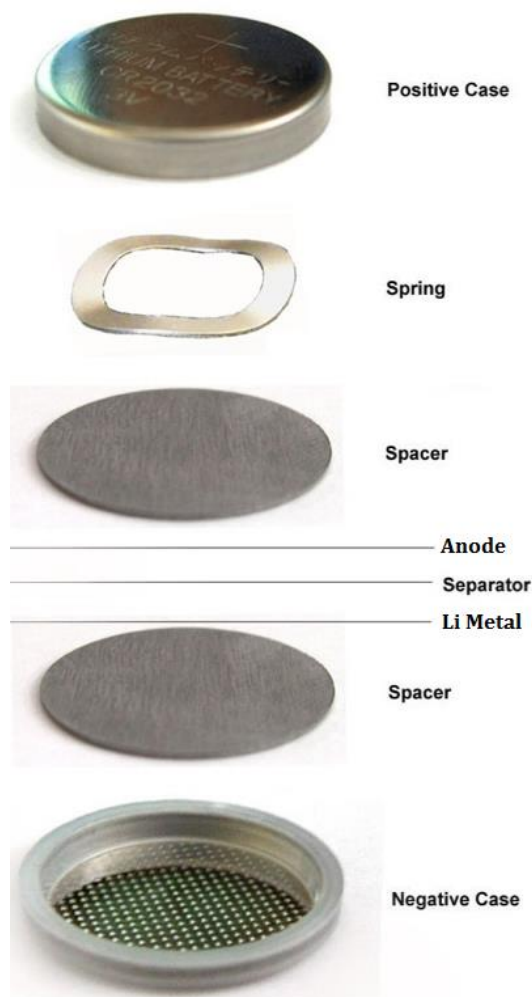
Fig 4.2 Diagram of 2032 type coin half-cell assembly.

4.4 Physical and structural characterizations

4.4.1 Scanning Electron Microscopy (SEM)

Scanning Electron Microscopy was used for two purposes namely for observing the morphology of the silicon particles after (i) etching and (ii) carbon coating on the etched silicon particles.

The etched silicon powders were sputter coated with a thin layer of gold before doing the SEM using Edwards sputter Coater to avoid charging of the samples. For this study, the microscopic investigations were performed using Hitachi S-4800 Field Emission Scanning Electron Microscope at room temperature. The voltage used for taking the images was set to 20kV.

4.4.2 X-ray diffraction (XRD)

X-ray diffraction (XRD) is an analytical technique primarily used for phase identification of a crystalline material besides the structure of the material. The X-ray diffraction was taken on samples of polycrystalline silicon and carbon coated porous silicon particles for analyzing the phases present, if any and the purity of the samples.

In this study, XRD experiments were performed using a Bruker AXS D8 Discover X-ray Diffractometer with CuK_{α} radiation at room temperature. The experiment was interfaced with the software of Pilot. The ranges of 2θ covered was set between 10 and 90 degree, for the diffraction experiments.

4.4.3 Raman spectroscopy

Raman spectroscopy is a spectroscopic technique used to analyze vibrational, rotational, and other low-frequency modes in a system by inelastic scattering of monochromatic laser. For analyzing the carbon-based materials Raman Spectroscopy is very suitable as an effective and powerful characterization technique, because it is sensitive to the different bands. It is often used to detect the quality of carbon (i.e. graphitization), which is an important factor for Li intercalation/de-intercalation and hence electrochemical properties.

In this study, Raman spectroscopy measurements were carried out using a Nicolet Almega XR Dispersive Raman 960 spectrometer with 532 nm laser excitation over the range 140-2000 cm^{-1}

at 80% of incident laser power (max power: 150mW). A collection time of 30s was used for each spectrum and for each acquisition 20 spectra were accumulated in order to reduce noise and avoid CCD saturation. To analyze the Raman spectra, the peaks were fitted using 'Peak Fit' software after linear background subtraction.

4.5 Electrochemical characterizations

4.5.1 Galvanostatic charge/discharge cycling test

Galvanostatic charge/discharge cycling test is a method used at a constant current to charge and discharge the coin cell over a voltage range to get the cycling performance of the electrochemical cell. Besides this, galvanostatic charge/discharge cycling test can also provide an important information on the coulombic efficiency, which means the efficiency of transferring amount of charge during intercalation/de-intercalation in a cell facilitating an electrochemical reaction.

In this study, battery cycling was performed using a MACCOR battery tester (4300 M). The voltage cutoff was set to 1.5V and 1mV versus Li/Li$^+$, and the cycling current was set to 500μAcm^{-2} for 50 cycles.

4.5.2 Cyclic Voltammetry (CV) test

Cyclic voltammetry (CV) is an electrochemical measurement, which measures the current change under a constant applied voltage over a specific voltage range during charge-discharge and number of cycles. CV is primarily used for analyzing the electrode processes, especially the electron-transfer reaction and electro-chemical reaction like formation of Solid Electrolyte Interphase (SEI).

In this study, cyclic voltammetry measurements were conducted using a potentiostat (Princeton Applied Research, VersaSTAT 4) between 2V and 1mV at a scan rate of 1mV/s and the cycle number was set to 20.

4.5.3 Electrochemical impedance spectroscopy (EIS)

Electrochemical impedance spectroscopy is a technique to measure the impedance of an electrochemical device over a range of frequencies. In the present study, EIS measurements were

34

carried out using the same instrument that was used for cyclic voltammetry measurements (Princeton Applied Research, VersaSTAT 4), and the frequency range was set as 1MHz to 10mHz.

CHAPTER V

RESULTS AND DISCUSSION

5.1 Processing of silicon based anode

5.1.1 Morphology of etched silicon

The pristine micron size polycrystalline particles of silicon (metallurgical grade) were etched using a metal assisted chemical etching (MACE) method as described in methodology section. Also, to check the morphology of etched silicon, the SEM test was done of these particles as mentioned in methodology section too. The SEM pictures of resulting etched particles with silicon nanostructures are shown in Fig. 5.1.

The as received polycrystalline silicon powders with large polydispersity can be observed from the SEM image as shown in Fig. 5.1 (a). The sizes of the particles range from few micron to 100μm with smooth surface as can be seen from Fig. 5.1 (b). However, after etching, the surfaces of the silicon particles become porous with very thin hair like nanowires (Fig. 5.1 (c)) or some hierarchical nanostructures. It is to be noted that metal assisted chemical etching creates all these structures on the surface of each of the particles but the core remains un-etched. The silicon nanowires as shown in Fig. 5.1 (c and d), are uniformly distributed on the particle surface almost in the same vertical direction. There are spaces between the silicon nanowires can be observed from the Fig. 5.1 (d). The advantage of MACE for creating nanowires is that it creates void spaces between the wires during etching, which could help in accommodating large volume expansion during lithiation of silicon.
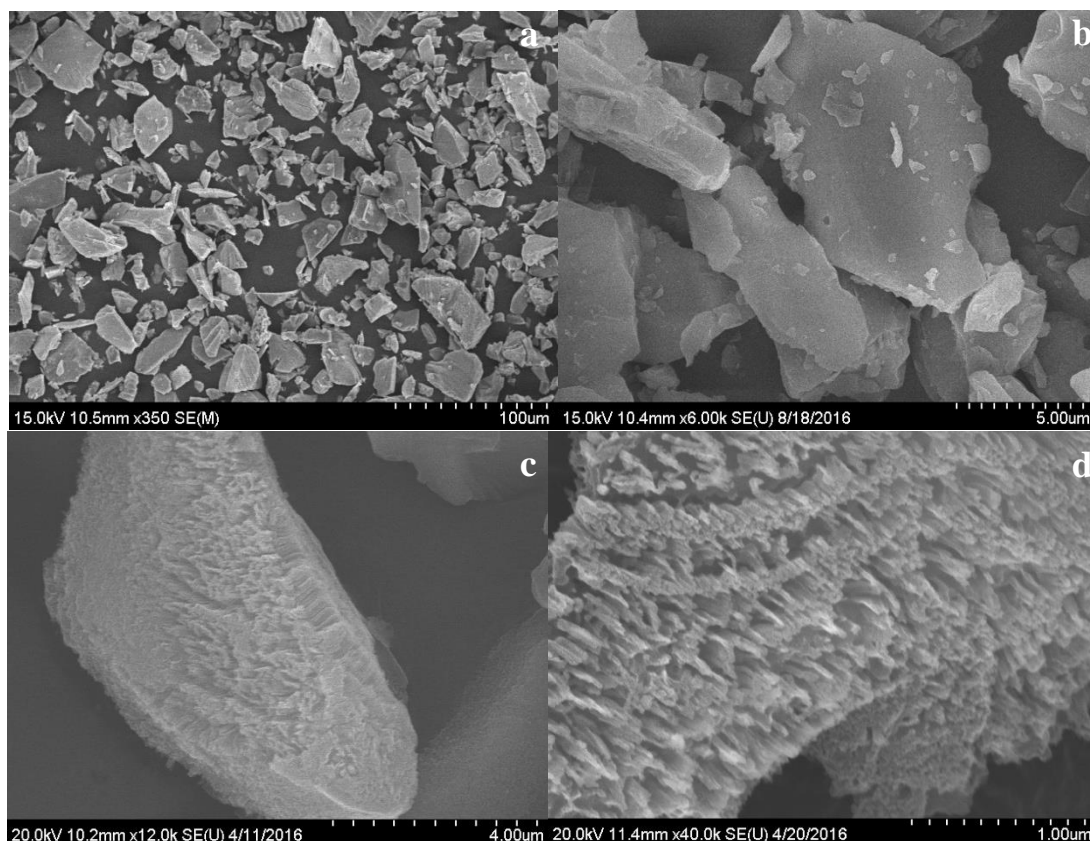
Fig 5.1 Typical morphology of polycrystalline silicon particles (a, b) before etching, and (c, d) after etching at two different magnifications.

5.1.2 Carbon coating on etched silicon particles

Coating on individual particles is always a big challenge. So, to achieve a uniform coating on each individual particle, the etched silicon particles were separated by some super conductive nanoparticles in a solution of furfuryl alcohol which itself act as a precursor for carbon coating and then gelled the polymeric solution suddenly so that all dispersed etched particles become frozen. Thus, we could achieve a structure uniformly distributed within the polymer matrix. By this process some of the porous regions surrounding the nanowires on silicon particles may be filled with the super conducting carbon black, which could help in getting better connection between the active silicon surfaces besides separating them in the polymeric (furfuryl alcohol in this study) solution. After uniformly dispersing the mixture in fufuryl alcohol (FFA) by using

sonication, hydrochloric acid (HCl) was used to polymerize it, which freezes the structure rapidly.

Finally, the gelled dried sample was pyrolyzed as mentioned in the earlier section of experimental

procedure. Pyrolyzing at a temperature of 750°C creates coating of carbon primarily on the etched

silicon structures.

The XRD patterns taken from the raw polycrystalline silicon powder vs. XRD pattern taken from

carbon coated silicon sample show the appearance of extra peak corresponding to carbon after

coating (Fig. 5.2). Both the XRD pattern shown in Fig. 5.2 correspond to the peaks coming from

silicon and no other trace was found except an extra carbon peak in coated sample.
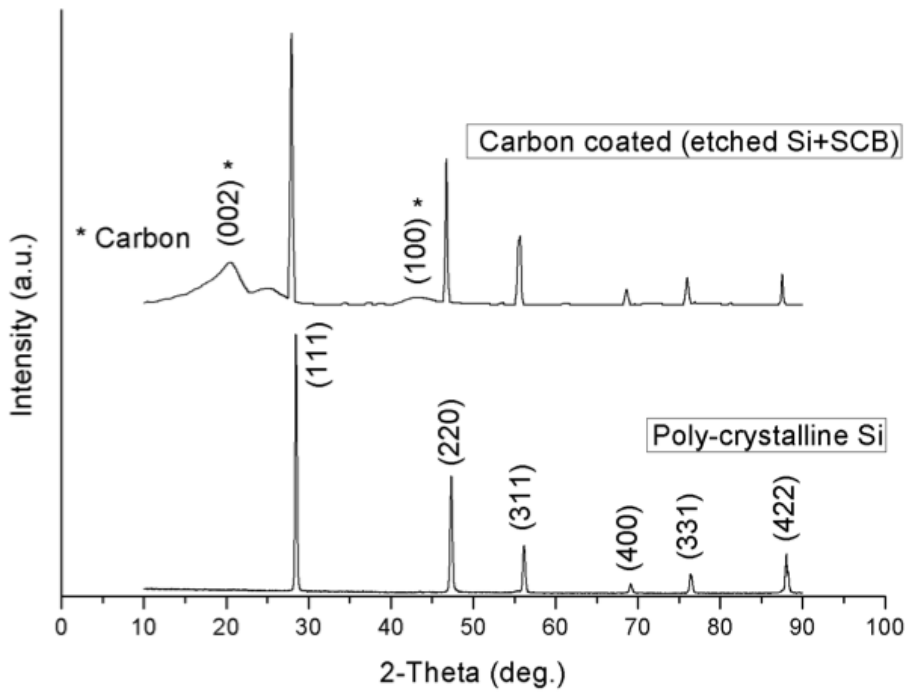
Fig 5.2 X-ray diffraction pattern of the carbon coated etched silicon networked with superconducting carbon black and the raw polycrystalline silicon powder as a reference.

To check the quality of carbon coated on the etched silicon structures, the sample was

characterized using Raman spectroscopy. The Raman spectrum taken from the coated sample is

shown in Fig. 5.3. According to the figure, the overall higher intensity of the peak coming from

silicon at ~522cm^{-1} indicates that most of the underlying material is still silicon and lesser amount

of carbonaceous material, indicating the possibility of a thin layer of carbon on the etched silicon structures or from superconducting carbon. It should be mentioned that Raman spectroscopy is a surface sensitive characterization technique and thus, the peak intensity coming from the carbonaceous phase is strong enough although less than the peak intensity coming from the underlying silicon.

The presence of defect (D) band and graphitic (G) band alone can be distinguished after deconvolution of the observed peaks. The red line curve represents the D band located at ~1334cm^{-1} and the blue line curve is associated with the G band, which appears at ~1598cm^{-1}. The strong presence of the peaks at 1334cm^{-1} and 1598cm^{-1} associated with the carbonaceous phase indicates the quality and coverage of the carbon coating. The higher intensity of the G band than the D band intensity indicates the fact that the carbon shells are mostly graphitic, which is desirable in our case as it can improve the conductivity and the reversible capacity of the electrode.
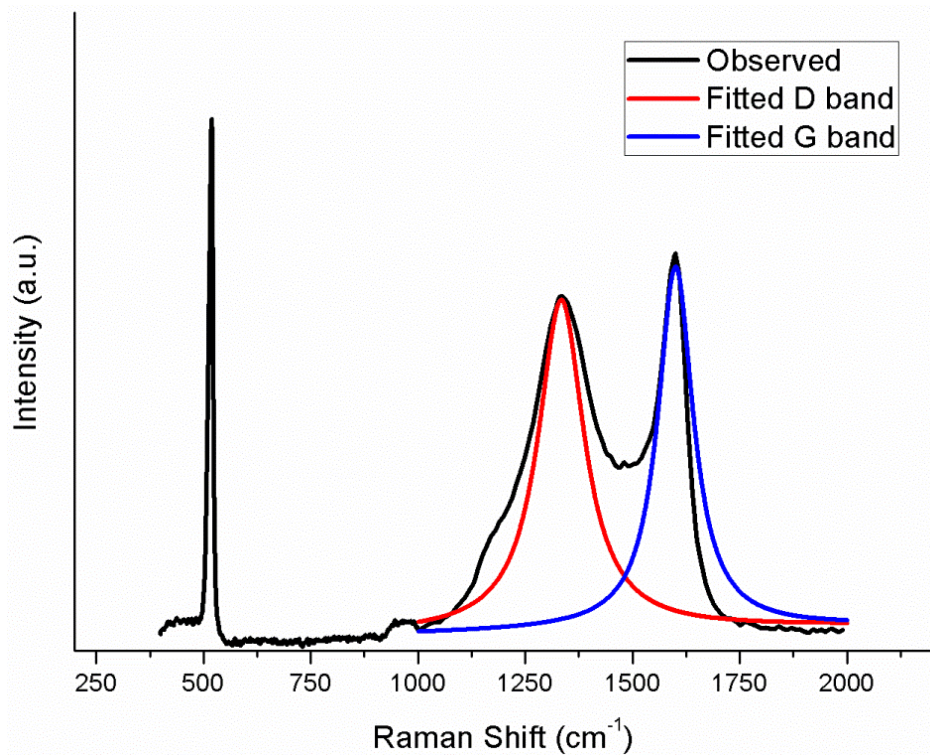
Fig 5.3 Raman spectra of the carbon coated etched silicon structures and fitted peaks.

5.2 Electrochemical performances

5.2.1 Cyclic Voltammetry (CV) test:

The electrochemical behaviors of anode made of carbon coated etched silicon (synthesized and processed as discussed in Chapter IV and earlier section of this chapter were tested on 2032 type coin cell and first analyzed by cyclic voltammetry (CV) as shown in Fig. 5.4. The cyclic voltammetry curve was taken at a scan rate of 1mV/s for 20 cycles as mentioned in methodology section (Chapter IV).
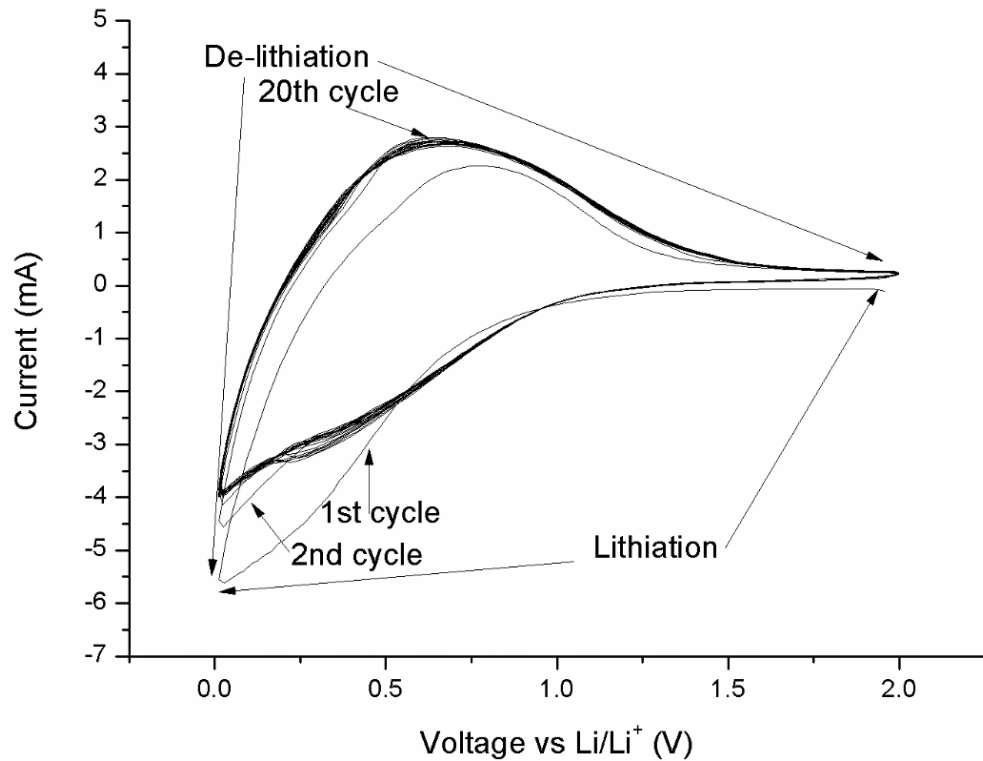
Figure 5.4 Cyclic voltammetry curves of the carbon coated of etched silicon structures.

The important fact about the coated CV curve is that it has no signature of peak corresponding to the formation of $Li_{15}Si_4$. It has been observed that lithiation of crystalline (c) silicon transforms it

to an amorphous (a) silicon, which means the Li_xSi alloy is amorphous in nature. However, during lithiation (intercalation) below a certain limit (usually below 50mV) it transforms into an alloy with a formula of $Li_{15}Si_4$, which is crystalline in nature [53, 74]. And if the silicon is allowed to over-lithiate to phase $Li_{22}Si_5$, its theoretical capacity will be 4200mAh/g, and this can happen if the crystalline phase of $Li_{15}Si_4$ transforms to amorphous phase of $Li_{22}Si_5$ as shown in Fig. 2.3 in Chapter II. With a variety of reports (sometimes contradictory to each other) this phase transformation (c-a-c) is reported to have detrimental effect on capacity retention [20, 53]. Few of the literature claims this to be the reason for fracture of silicon electrode besides the existing knowledge of about 400% volume expansion to be the primary reason for fracture [2]. It is also reported that this particular crystalline phase ($Li_{15}Si_4$), which would have detrimental effect in performance could be avoided by formation of nanostructures [75]. Although the synthesis and processing is not transforming the whole silicon particle into nanostructures but the outer surface consists of silicon nanowires. This could be the reason for the absence of peak corresponding to $Li_{15}Si_4$ in the CV curve of the etched silicon samples coated with carbon (Fig. 5.4). Thus, avoiding this particular phase during lithiation of crystalline silicon would result only in amorphous Li_xSi upon lithiation and then to amorphous silicon during de-lithiation cycles and lead to better cyclability as verified later from the galvanostatic charge-discharge cycles. However, for all the cycles of lithiation, the peak ends at about 0.01V corresponds to the alloying reaction between silicon and lithium. The anodic reactions in Fig. 5.4, shows one broad shoulder close to 0.5V, which may be ascribed to the de-lithiation from Li_xSi. The reproducibility of the coated sample can be related to the overlapping of the de-alloying curves as is clearly evident from Fig. 5.4.

5.2.2 Electrochemical Impedance Spectroscopy (EIS) test:

The electrochemical impedance spectroscopy (EIS) measurements were done for both the carbon coated samples as well as the pristine polycrystalline sample for reference. Figure. 5.5 shows the Nyquist plot from the EIS study. The resistive components (R_C, R_S, and R_E) calculated from the

intercepts of the semicircle are given in Table 5.1. The R_C is the contact resistance between electrode and copper substrate/current collector and R_S is the total resistance of the electrode and copper substrate/current collector, and $R_E=R_S-R_C$ is the effective electrode resistance [76]. The decrease in resistance of the coated sample in comparison to the pristine polycrystalline silicon is probably due to modification done by coating on individual etched silicon particles and the good contact between them as provided by the carbon coating as well as superconducting carbon black. Thus, this new way of processing helps in improving the total conductivity of the cell and provides stability of the active material against the huge volume expansion during lithiation, which results in high reversible capacity even after 50 cycles (discussed later). Further optimization of the electrodes and associated assembly by lowering resistance is expected to further decrease the capacity loss.
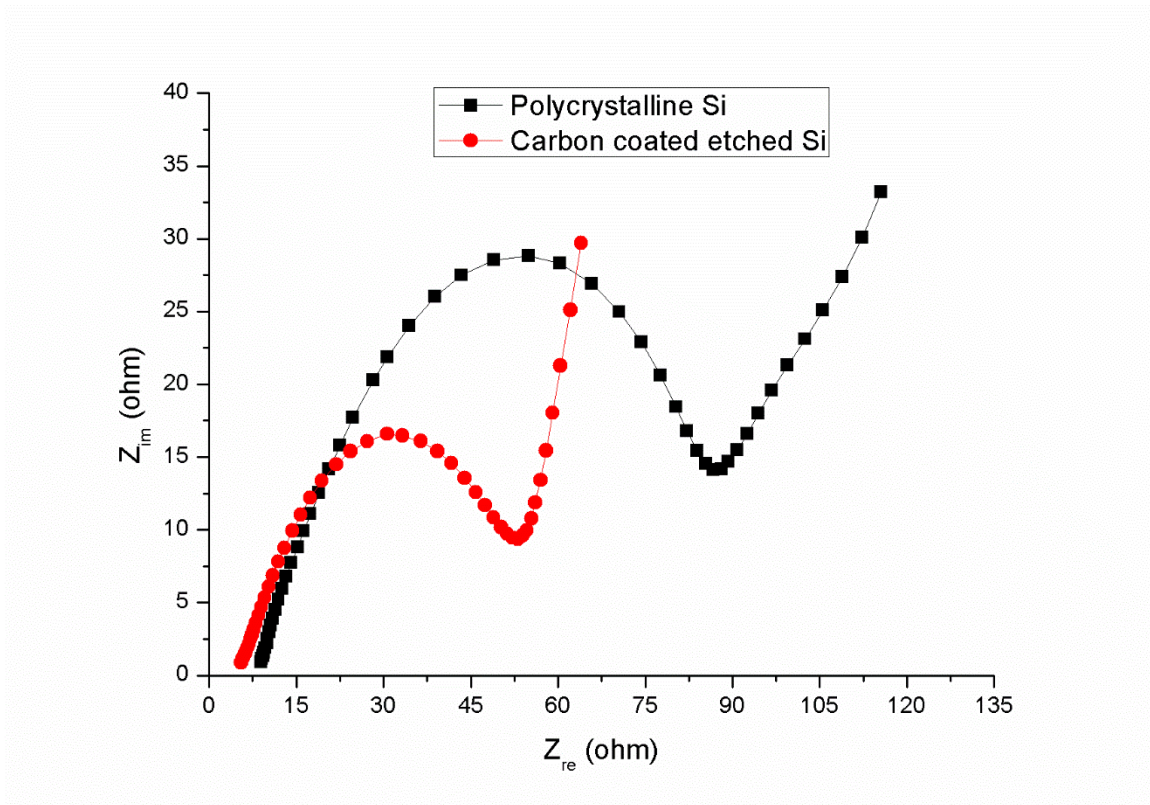
Figure 5.5 Nyquist plots of polycrystalline silicon Vs. etched silicon with carbon coating.

Table 5.1 Calculated electrode resistance from the Nyquist plots.

Sample	Contact Resistance R$_C$ (ohm)	Total Resistance, R$_S$ (ohm)	Net Electrode Resistance, R$_E$ (ohm)
Polycrystalline Si	5.9	101.8	95.9
Carbon coated etched Si	4.5	69.3	64.8

5.2.3 Charge-discharge (cycling) performance:

Charge-discharge curves for the carbon coated etched silicon sample is shown in Figure. 5.6.
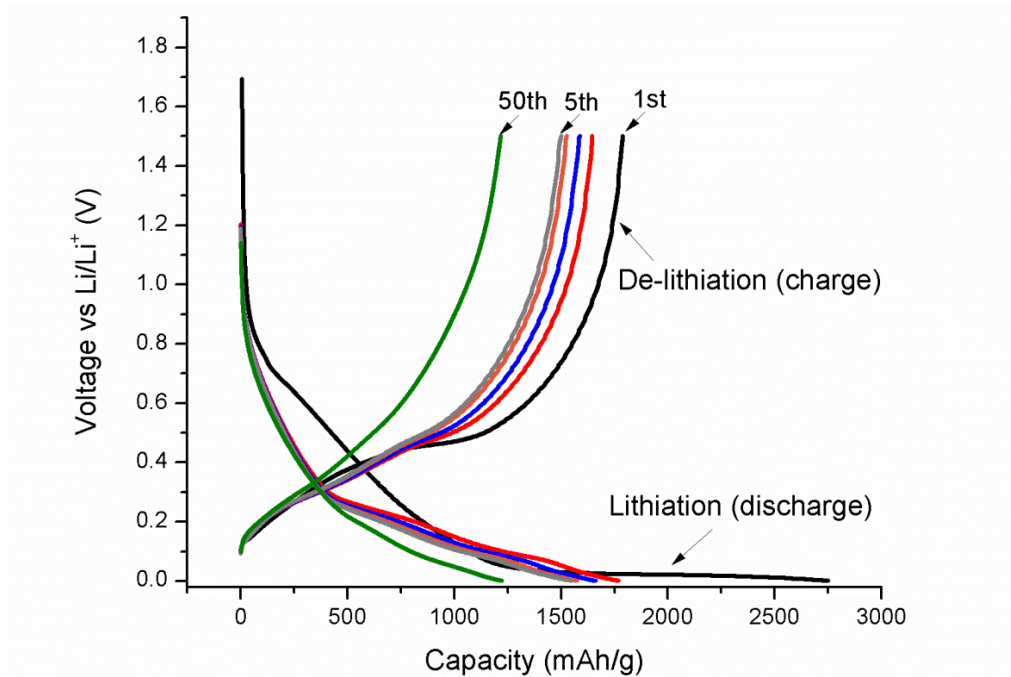
Figure 5.6 Charge-discharge curves for the carbon coated silicon sample up to 50 cycles.

The first lithiation cycle (discharge) specific capacity of carbon coated silicon sample is about 2750mAh/g as can be observed from Fig. 5.6. A long and gradual increase in the slope starting at ~0.1V (Fig. 5.6, 1st lithiation cycle) is characteristic of alloying reaction between lithium and host

silicon matrix. Subsequent lithiation curves show a slope starting at ~0.3V (Fig. 5.6, 2nd cycle onwards), probably as a result of lithiation of the amorphous silicon [74].

Figure. 5.7 shows the cycle performances of the carbon coated etched silicon sample along with the pristine and etched polycrystalline silicon sample.
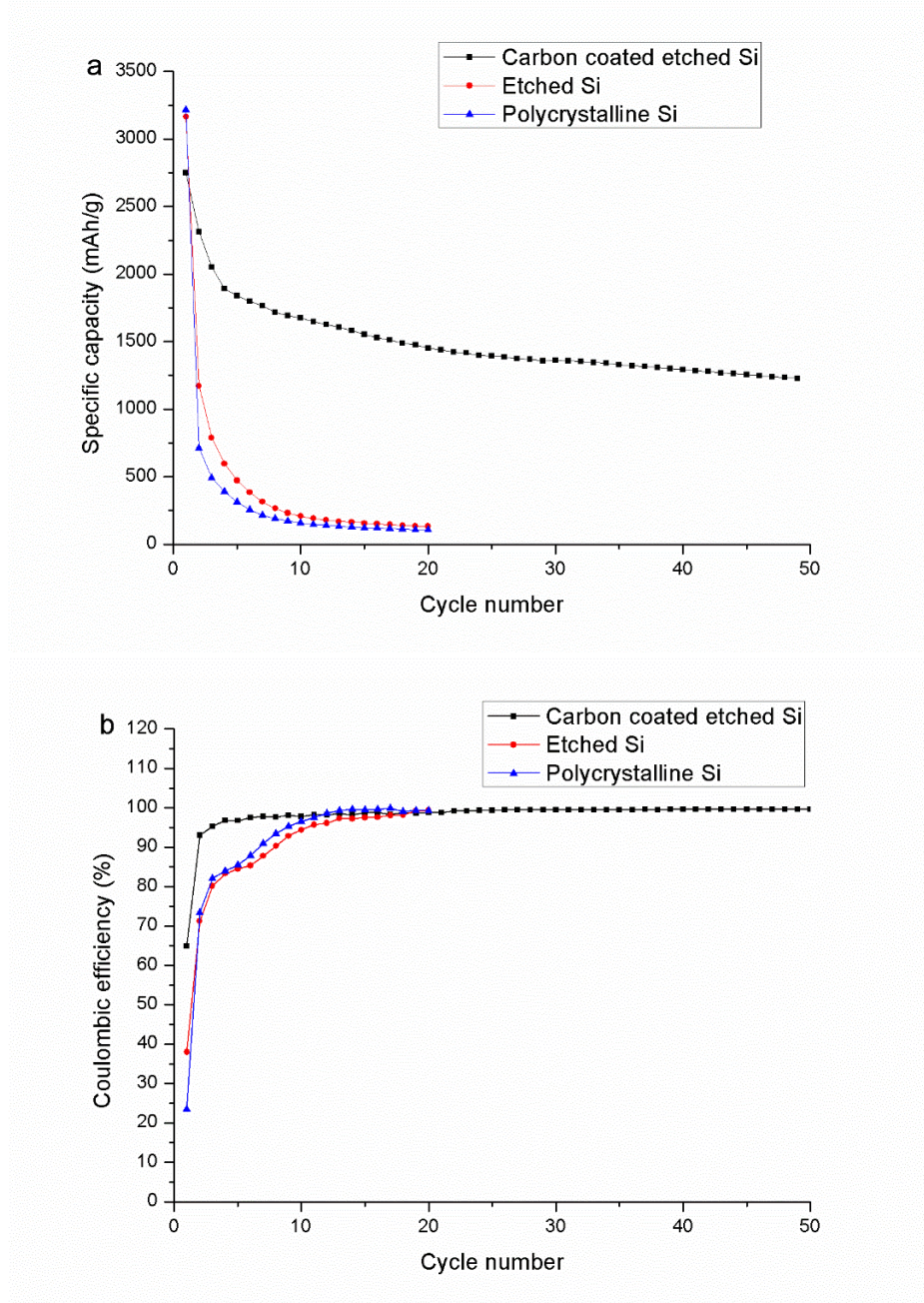
Figure 5.7. (a) Specific capacity Vs. cycle numbers, and (b) Coulombic efficiency of the coated silicon sample along with pristine and etched polycrystalline silicon sample for reference.

44

It can be seen from Fig. 5.7 that compared to the pristine polycrystalline silicon sample which has the highest lithiation specific capacity of ~3214mAh/g and etched silicon sample of ~3116mAh/g (as shown in Fig. 5.7 (a)), the coated silicon sample has relatively lower first cycle specific capacity, probably due to the presence of carbonaceous material, which is supposed to have lower specific capacity than silicon. But the capacities are still much higher than the commercial graphite anode (theoretical capacity of 372mAh/g).

The high initial specific capacity is an indication of major participation of silicon within the carbonaceous network. The carbon coated silicon electrode structure shows improved cyclability, when compared to pristine polycrystalline silicon sample or etched silicon sample, which have lost almost all their capacity even after initial few cycles. The worse cycle life in terms of capacity fading for the pristine polycrystalline sample is probably due to the fracture and subsequently detachment from each other and from the current collector as well. It should be remembered that for making the pristine silicon based electrode, we have not followed the steps for avoiding agglomeration and coating. The coated sample was processed by rapidly freezing the mixture of superconductive carbon black and etched porous silicon in polymeric solution, which created electrically well-connected nanostructure electrode. Upon pyrolyzing, the frozen polymeric gel produced carbon coating on individually etched silicon particles. The failure of raw polycrystalline sample is quite obvious due to its fracture, which is unavoidable for the large micron size of pristine silicon particles during the lithiation/ delithiation. Even after etching, the sample failed probably due to the isolation caused by the fracture from the un-etched core silicon. The improved performance and capacity retention of the coated silicon sample can be attributed to the newly adopted processing of the electrode. In this approach, a uniform electrical connectivity was achieved by the superconducting carbon black (SCB) and carbon coating during the processing step in which rapid freezing by gelation of the FFA by HCl created the uniformly mixed individual phases. It should be noted that even coating cannot be effective if there is agglomeration of particles, which could behave as a bulk and upon fracture will not have any

connection as provided by both the SCB and coated carbon on etched silicon particles. The porous structure, which may have filled with and separated by SCB and then coated with thin layers of carbon also improves the stability of SEI layer formation. The controlled and uniform SEI layer can also contribute to improved reversible capacity. Uncontrolled growth of SEI is a secondary issue for bulk silicon. SEI forms on the newly exposed surfaces resulting from the fractured surfaces from successive cycles and hinders the diffusion of ions into the active material. Here in this study the outer layer of carbon helps in controlled formation of SEI as the reaction happens on the surface of the particles. Also, the outer layer of carbon present in this case is more graphitic (as indicated by Raman spectrum) and lithium ion has the ability to intercalate/de-intercalate through graphitic layers reversibly and is a stable host for lithium ions. Thus, all the carbon structures inside and outside will allow lithium to diffuse inside to enter into the silicon lattice and the high surface areas created by etching and from the silicon nanowires will be available for intercalation.

Figures. 5.7 (a) and (b) show the high improved reversible capacity with high coulombic efficiency for carbon coated etched silicon sample, especially after a few initial cycles. The first cycle coulombic efficiency of the coated sample is near 65%, which is much higher than the raw polycrystalline sample, which has 23%, and etched sample with 38%. But only after 5 cycles, the coulombic efficiency of coated sample has reached to more than 99%. Thus, the improvement in capacity retention can be clearly observed from these figures. For carbon coated silicon sample, the subsequent charge/discharge cycles maintained improved coulombic efficiency (99.6%) with a reversible capacity of ~1222mAh/g even after 50 cycles. From these results, the carbon coating method ensures that the pores or voids available between the etched silicon particles are filled with superconductive carbon black nanoparticles (which has varied dimension in nano-metric level). This may provide the conducting path even after fracture of Si thereby enhancing the conductivity of the active anode materials, which is required for getting high discharge capacity even after many number of cycles. Not only that, the conformal and uniform conducting carbon

coating on individual silicon particles, which is achieved by avoiding agglomeration during previous step of sudden gelation also provides a stable and flexible cover. This approach also controls the amount of SEI formation without which there would have been a successive loss in capacity when the silicon particles fracture and create new surfaces for additional formation of the SEI layer. The presence of enhanced number of reversible sites for intercalation in carbon-based anode materials also depends on the level of graphitization. It has been reported that increased defects result in increased irreversible capacity by providing more sites for lithium ions. The lower value of the ratio I_d/I_g in Raman spectra of our study also indicates formation of more graphitic phase in the coating thereby facilitating easy path through the graphitic layer of lithium towards silicon anode during lithiation and delithiation steps.

CHAPTER VI

CONCLUSIONS

This study explores the possibility of silicon based anode as a promising candidate for lithium-ion batteries through novel way of processing. The cost-effective processing approach utilized a metallurgical grade polycrystalline silicon and then a chemical etching method was used for creating silicon nanostructures. These steps were followed by carbon coating of the nanostructures for ensuring uniform coating on the individual porous silicon particles, which provided both the conductive and flexible paths for relaxation during volume expansion. The following conclusions can be drawn from this study.

1. The new processing approach not only provided channels for fast electronic and ionic transfer from superconductive carbon, but also helped in avoiding agglomeration of the etched silicon particles when adding the HCl to freeze them suddenly, which was a primary obstacle for coating individual particles.

2. The outer layer coating of carbon on silicon, also controlled the SEI formation for improving performance.

3. Avoiding the formation of metastable $c\text{-}Li_{15}Si_4$ phase by creating the nanowires upon etching helped in getting better stability and cycle life of silicon anode.

4. The EIS study indicated that the carbon coated porous silicon has lower resistance and higher conductivity, which helped to get high reversible capacity and long lifetime.

5. In this study, the carbon coated porous silicon half-cell showed an impressive initial specific discharge capacity of approximately 2750mAh/g and a reversible capacity of ~1222mAh/g after 50 cycles with a very high coulombic efficiency of 99.6%.

6. These results confirmed that silicon is a promising anode material for next generation high capacity lithium-ion batteries.

CHAPTER VII

SUGGESTIONS FOR FUTURE RESEARCH

Although in this work, we achieved pretty good electrochemical performances of the silicon based anode material based on robust synthesis route/processing, but there is huge scope for further improvement. There are two important directions that can be pursued in future to improve the performance of the anode.

The first approach could be improving the etching process. Two problems that exist in this process. One is the uniform etching on each and every particle so as to get a homogeneous nanostructure. The other one is the extent of etching through thickness so as to consume the whole particle mass and convert it into only silicon nanostructures with as minimum as possible unreacted core or volume. As the SEM images of the etched silicon particles show the etching has happened only on the silicon surface and the length of silicon nanowires is too long.

Another research direction could be optimizing the weight ratio of silicon to carbon as well as controlling the quality and thickness of the carbon coating step to control the carbon coating.

REFERENCES

[1]   David Linden; Reddy, T. B. *Handbook of Batteries*; 2004.

[2]   Dash, R.; Pannala, S. Theoretical Limits of Energy Density in Silicon-Carbon Composite Anode Based Lithium Lon Batteries. *Sci. Rep.* **2016**, *6* (February), 27449.

[3]   Tarascon, J.-M.; Armand, M. Issues and Challenges Facing Rechargeable Lithium Batteries. *Nature, Publ. online 15 Novemb. 2001; | doi10.1038/35104644* **2001**, *414* (6861), 359.

[4]   Transparency Market Research. Lithium-ion Battery Market – Growing Use of Low Power Capacity Lithium-ion Batteries in Consumer Electronics – satPRnews http://www.satprnews.com/2017/01/16/lithium-ion-battery-market-growing-use-of-low-power-capacity-lithium-ion-batteries-in-consumer-electronics/ (accessed Mar 27, 2017).

[5]   Nitta, N.; Wu, F.; Lee, J. T.; Yushin, G. Li-Ion Battery Materials: Present and Future. *Mater. Today* **2015**, *18* (5), 252–264.

[6]   Basu, S.; Zeller, C.; Flanders, P. J.; Fuerst, C. D.; Johnson, W. D.; Fischer, J. E. Synthesis and Properties of Lithium-Graphite Intercalation Compounds. *Mater. Sci. Eng.* **1979**, *38* (3), 275–283.

[7]   Goriparti, S.; Miele, E.; De Angelis, F.; Di Fabrizio, E.; Proietti Zaccaria, R.; Capiglia, C. Review on Recent Progress of Nanostructured Anode Materials for Li-Ion Batteries. *J. Power Sources* **2014**, *257*, 421–443.

[8]   Yang, J.; Zhou, X. Y.; Li, J.; Zou, Y. L.; Tang, J. J. Study of Nano-Porous Hard Carbons as Anode Materials for Lithium Ion Batteries. *Mater. Chem. Phys.* **2012**, *135* (2–3), 445–450.

[9]   Bridges, C. A.; Sun, X. G.; Zhao, J.; Paranthaman, M. P.; Dai, S. In Situ Observation of Solid Electrolyte Interphase Formation in Ordered Mesoporous Hard Carbon by Small-Angle Neutron Scattering. *J. Phys. Chem. C* **2012**, *116* (14), 7701–7711.

[10]   Fu, L. J.; Liu, H.; Li, C.; Wu, Y. P.; Rahm, E.; Holze, R.; Wu, H. Q. Surface Modifications of Electrode Materials for Lithium Ion Batteries. *Solid State Sci.* **2006**, *8* (2), 113–128.

[11]   Meunier, V.; Kephart, J.; Roland, C.; Bernholc, J. Ab Initio Investigations of Lithium Diffusion in Carbon Nanotube Systems. **2002**, *88*.

[12]   Zhao, J.; Buldum, A.; Han, J.; Ping Lu, J. First-Principles Study of Li-Intercalated Carbon Nanotube Ropes. *Phys. Rev. Lett.* **2000**, *85* (8), 1706–1709.

[13]   Hou, J.; Shao, Y.; Ellis, M. W.; Moore, R. B.; Yi, B. Graphene-Based Electrochemical Energy Conversion and Storage: Fuel Cells, Supercapacitors and Lithium Ion Batteries. *Phys. Chem. Chem. Phys.* **2011**, *13* (34), 15384.

[14]   Chen, Z.; Belharouak, I.; Sun, Y. K.; Amine, K. Titanium-Based Anode Materials for Safe Lithium-Ion Batteries. *Adv. Funct. Mater.* **2013**, *23* (8), 959–969.

[15]   Szczech, J. R.; Jin, S.; Koller, S.; Raimann, P. R.; Woehrle, T.; Wurm, C.; Winter, M.; Zhang, Z.; Tarascon, J.-M.; Park, W. I.; Zang, D. S.; Kim, H.; Huang, Y.; Hwang, K.-C.; Rogers, J. A.; Paik, U. Nanostructured Silicon for High Capacity Lithium Battery Anodes. *Energy Environ. Sci.* **2011**, *4* (1), 56–72.

[16]   Rudawski, N. G.; Yates, B. R.; Holzworth, M. R.; Jones, K. S.; Elliman, R. G.; Volinsky, A. A. *Ion Beam-Mixed Ge Electrodes for High Capacity Li Rechargeable Batteries*; 2013; Vol. 223.

[17]   Chockla, A. M.; Klavetter, K. C.; Mullins, C. B.; Korgel, B. A. Solution-Grown Germanium Nanowire Anodes for Lithium-Ion Batteries. *ACS Appl. Mater. Interfaces* **2012**, *4* (9), 4658–4664.

[18]   Bruce, P. G.; Scrosati, B.; Tarascon, J.-M. Nanomaterials for Rechargeable Lithium Batteries. *Angew. Chemie Int. Ed.* **2008**, *47* (16), 2930–2946.

[19]   Park, C.-M.; Kim, J.-H.; Kim, H.; Sohn, H.-J.; Tarascon, J.-M.; Heier, K. R.; Chen, L.; Seshadri, R.; Stucky, G. D.; Dillon, A. C. Li-Alloy Based Anode Materials for Li Secondary Batteries. *Chem. Soc. Rev.* **2010**, *39* (8), 3115.

[20]   Wang, Z.; Zhou, L.; Lou, X. W. Metal Oxide Hollow Nanostructures for Lithium-Ion Batteries. *Adv. Mater.* **2012**, *24* (14), 1903–1911.

[21]   Yang, J.; Takeda, Y.; Imanishi, N.; Capiglia, C.; Xie, J. Y.; Yamamoto, O. SiO_x-Based Anodes for Secondary Lithium Batteries. *Solid State Ionics* **2002**, *152–153*, 125–129.

[22]   Jiang, J.; Li, Y.; Liu, J.; Huang, X.; Yuan, C.; Lou, X. W. Recent Advances in Metal Oxide-Based Electrode Architecture Design for Electrochemical Energy Storage. *Adv. Mater.* **2012**, *24* (38), 5166–5180.

[23]   Prosini, P. P.; Carewska, M.; Loreti, S.; Minarini, C.; Passerini, S. Lithium Iron Oxide as Alternative Anode for Li-Ion Batteries. *Int. J. Inorg. Mater.* **2000**, *2* (4), 365–370.

[24]   Ji, L.; Lin, Z.; Alcoutlabi, M.; Zhang, X.; Xun, S.; Lin, E.; Battaglia, V.; Zhang, Y.; Yasuda, K.; Dillon, A. C.; Liu, D. G.; Liu, J.; Rolison, D. R.; Sands, T.; Shi, L.; Sholl, D.;

Wu, Y. Y. Recent Developments in Nanostructured Anode Materials for Rechargeable Lithium-Ion Batteries. *Energy Environ. Sci.* **2011**, *4* (8), 2682.

[25]   Lai, C.-H.; Lu, M.-Y.; Chen, L.-J.; Lu, S. Y.; Wang, Z. L.; Gao, Z. Y.; Hao, Y.; Chen, L. J.; Wang, Z. L.; Yang, X.; Zhu, J. Metal Sulfide Nanostructures: Synthesis, Properties and Applications in Energy Conversion and Storage. *J. Mater. Chem.* **2012**, *22* (1), 19–30.

[26]   Boyanov, S.; Annou, K.; Villevieille, C.; Pelosi, M.; Zitoun, D.; Monconduit, L. Nanostructured Transition Metal Phosphide as Negative Electrode for Lithium-Ion Batteries. *Ionics (Kiel).* **2008**, *14* (3), 183–190.

[27]   Marom, R.; Amalraj, S. F.; Leifer, N.; Jacob, D.; Aurbach, D. A Review of Advanced and Practical Lithium Battery Materials. *J. Mater. Chem.* **2011**, *21* (27), 9938.

[28]   Nazri, G.; Pistoia, G. (Gianfranco). *Lithium Batteries : Science and Technology*; Springer, 2009.

[29]   Girishkumar, G.; McCloskey, B.; Luntz, A. C.; Swanson, S.; Wilcke, W. Lithium-Air Battery: Promise and Challenges. *J. Phys. Chem. Lett.* **2010**, *1* (14), 2193–2203.

[30]   Scrosati, B.; Garche, J. Lithium Batteries: Status, Prospects and Future. *J. Power Sources* **2010**, *195* (9), 2419–2430.

[31]   Evanoff, K.; Khan, J.; Balandin, A. A.; Magasinski, A.; Ready, W. J.; Fuller, T. F.; Yushin, G. Towards Ultrathick Battery Electrodes: Aligned Carbon Nanotube - Enabled Architecture. *Adv. Mater.* **2012**, *24* (4), 533–537.

[32]   Oktaviano, H. S.; Yamada, K.; Waki, K.; Yoshida, N.; Kim, D. Y.; Yamada, Y.; Noda, S.; Yamada, A.; Horn, Y. S.; Yamashita, J.; Don, F.; Hata, K.; Hatori, H. Nano-Drilled Multiwalled Carbon Nanotubes: Characterizations and Application for LIB Anode Materials. *J. Mater. Chem.* **2012**, *22* (48), 25167.

[33] Li, H.; Zhou, H.; Takei, K.; Shigemura, H.; Tabuchi, M.; Kageyama, H.; Iwahoria, T.; Jo, M. H.; Markovsky, B.; Aurbach, D. Enhancing the Performances of Li-Ion Batteries by Carbon-Coating: Present and Future. *Chem. Commun.* **2012**, *48* (9), 1201–1217.

[34] Wagemaker, M.; Mulder, F. M. Properties and Promises of Nanosized Insertion Materials for Li-Ion Batteries. *Acc. Chem. Res.* **2013**, *46* (5), 1206–1215.

[35] Moretti, A.; Kim, G.-T.; Bresser, D.; Renger, K.; Paillard, E.; Marassi, R.; Winter, M.; Passerini, S. Investigation of Different Binding Agents for Nanocrystalline Anatase TiO_2 Anodes and Its Application in a Novel, Green Lithium-Ion Battery. *J. Power Sources* **2013**, *221*, 419–426.

[36] Li, X.; Wang, C.; Chen, C. H.; Xie, S.; Cao, X. Q.; Ma, Y.; Yao, J. N.; Gu, C. D.; Zhang, X. W.; Kang, F. Y.; Fan, H. J.; Verbrugge, M. Engineering Nanostructured Anodes via Electrostatic Spray Deposition for High Performance Lithium Ion Battery Application. *J. Mater. Chem. A* **2013**, *1* (2), 165–182.

[37] Zhu, G.-N.; Chen, L.; Wang, Y.-G.; Wang, C.-X.; Che, R.-C.; Xia, Y.-Y. Binary $Li_4Ti_5O_{12}$-$Li_2Ti_3O_7$ Nanocomposite as an Anode Material for Li-Ion Batteries. *Adv. Funct. Mater.* **2013**, *23* (5), 640–647.

[38] Meng, X.; Banis, M. N.; Geng, D.; Li, X.; Zhang, Y.; Li, R.; Abou-Rachid, H.; Sun, X. Controllable Atomic Layer Deposition of One-Dimensional Nanotubular TiO_2. *Appl. Surf. Sci.* **2013**, *266*, 132–140.

[39] Xu, J.; Zhu, Y. Monodisperse Fe_3O_4 and γ-Fe_2O_3 Magnetic Mesoporous Microspheres as Anode Materials for Lithium-Ion Batteries. **2012**, 2–7.

[40]   Barreca, D.; Cruz-Yusta, M.; Gasparotto, A.; MacCato, C.; Morales, J.; Pozza, A.; Sada, C.; Sánchez, L.; Tondello, E. Cobalt Oxide Nanomaterials by Vapor-Phase Synthesis for Fast and Reversible Lithium Storage. *J. Phys. Chem. C* **2010**, *114* (21), 10054–10060.

[41]   Zhang, L.; Hu, P.; Zhao, X.; Tian, R.; Zou, R.; Xia, D.; Liu, H. K.; Dou, S. X. Controllable Synthesis of Core–shell Co@CoO Nanocomposites with a Superior Performance as an Anode Material for Lithium-Ion Batteries. *J. Mater. Chem.* **2011**, *21* (45), 18279.

[42]   Paolella, A.; Brescia, R.; Prato, M.; Povia, M.; Marras, S.; Trizio, L. De. Colloidal Synthesis of Cuprite (Cu_2O) Octahedral Nanocrystals and Their Electrochemical Lithiation. **2013**, 1–11.

[43]   Li, J.; Xiong, S.; Li, X.; Qian, Y.; Zhang, L. Z.; Kim, D. K.; Kang, K.; Lou, X. W.; Cheng, H. M. A Facile Route to Synthesize Multiporous $MnCo_2O_4$ and $CoMn_2O_4$ Spinel Quasi-Hollow Spheres with Improved Lithium Storage Properties. *Nanoscale* **2013**, *5* (5), 2045.

[44]   Aravindan, V.; Suresh Kumar, P.; Sundaramurthy, J.; Ling, W. C.; Ramakrishna, S.; Madhavi, S. Electrospun NiO Nanofibers as High Performance Anode Material for Li-Ion Batteries. *J. Power Sources* **2013**, *227*, 284–290.

[45]   Bhaskar, A.; Deepa, M.; Narasinga Rao, T. MoO_2/multiwalled Carbon Nanotubes (MWCNT) Hybrid for Use as a Li-Ion Battery Anode. *ACS Appl. Mater. Interfaces* **2013**, *5* (7), 2555–2566.

[46]   Liu, H.; Du, X.; Xing, X.; Wang, G.; Qiao, S. Z.; Peiro, F.; Cornet, A.; Morante, J. M.; Solovyov, L. A.; Tian, B. Z.; Bo, T.; Zhao, D. Y. Highly Ordered Mesoporous Cr_2O_3 Materials with Enhanced Performance for Gas Sensors and Lithium Ion Batteries. *Chem. Commun.* **2012**, *48* (6), 865–867.

[47] Reddy, A. L. M.; Gowda, S. R.; Shaijumon, M. M.; Ajayan, P. M. Hybrid Nanostructures for Energy Storage Applications. *Adv. Mater.* **2012**, *24* (37), 5045–5064.

[48] Zhang, W.-J. A Review of the Electrochemical Performance of Alloy Anodes for Lithium-Ion Batteries. *J. Power Sources* **2011**, *196* (1), 13–24.

[49] Goward, G. R.; Taylor, N. J.; Souza, D. C. S.; Nazar, L. F. The True Crystal Structure of $Li_{17}M_4$ (M=Ge, Sn, Pb)–revised from $Li_{22}M_5$. *J. Alloys Compd.* **2001**, *329* (1), 82–91.

[50] Liu, Y.; Hudak, N. S.; Huber, D. L.; Limmer, S. J.; Sullivan, J. P.; Huang, J. Y. In Situ Transmission Electron Microscopy Observation of Pulverization of Aluminum Nanowires and Evolution of the Thin Surface Al_2O_3 Layers during Lithiation-Delithiation Cycles. *Nano Lett.* **2011**, *11* (10), 4188–4194.

[51] Qian, J.; Qiao, D.; Ai, X.; Cao, Y.; Yang, H.; Yang, H.; Cui, Y. Reversible 3-Li Storage Reactions of Amorphous Phosphorus as High Capacity and Cycling-Stable Anodes for Li-Ion Batteries. *Chem. Commun.* **2012**, *48* (71), 8931.

[52] Darwiche, A.; Marino, C.; Sougrati, M. T.; Fraisse, B.; Stievano, L.; Monconduit, L. Better Cycling Performances of Bulk Sb in Na-Ion Batteries Compared to Li-Ion Systems: An Unexpected Electrochemical Mechanism. *J. Am. Chem. Soc.* **2012**, *134* (51), 20805–20811.

[53] Chan, C. K.; Peng, H.; Liu, G.; McIlwrath, K.; Zhang, X. F.; Huggins, R. A.; Cui, Y. High-Performance Lithium Battery Anodes Using Silicon Nanowires. *Nat. Nanotechnol.* **2008**, *3* (1), 31–35.

[54] Wu, H.; Cui, Y. Designing Nanostructured Si Anodes for High Energy Lithium Ion Batteries. *Nano Today* **2012**, *7* (5), 414–429.

[55]   Ryu, I.; Choi, J. W.; Cui, Y.; Nix, W. D. Size-Dependent Fracture of Si Nanowire Battery Anodes. *J. Mech. Phys. Solids* **2011**, *59* (9), 1717–1730.

[56]   Astrova, E. V.; Li, G. V.; Rumyantsev, A. M.; Zhdanov, V. V. Electrochemical Characteristics of Nanostructured Silicon Anodes for Lithium-Ion Batteries. *Semiconductors* **2016**, *50* (2), 276–283.

[57]   Xiao, Y.; Hao, D.; Chen, H. X.; Gong, Z. L.; Yang, Y. Economical Synthesis and Promotion of the Electrochemical Performance of Silicon Nanowires as Anode Material in Li-Ion Batteries. *ACS Appl. Mater. Interfaces* **2013**, *5* (5), 1681–1687.

[58]   Cui, L.-F.; Ruffo, R.; Chan, C. K.; Peng, H.; Cui, Y. Crystalline-Amorphous Core−Shell Silicon Nanowires for High Capacity and High Current Battery Electrodes. *Nano Lett.* **2009**, *9* (1), 491–495.

[59]   Peng, K.; Jie, J.; Zhang, W.; Lee, S.-T. Silicon Nanowires for Rechargeable Lithium-Ion Battery Anodes. *Appl. Phys. Lett.* **2008**, *93* (3), 33105.

[60]   Han, H.; Huang, Z.; Lee, W. Metal-Assisted Chemical Etching of Silicon and Nanotechnology Applications. *Nano Today* **2014**, *9* (3), 271–304.

[61]   Song, T.; Xia, J.; Lee, J. H.; Lee, D. H.; Kwon, M. S.; Choi, J. M.; Wu, J.; Doo, S. K.; Chang, H.; Park, W. Il; Zang, D. S.; Kim, H.; Huang, Y.; Hwang, K. C.; Rogers, J. A.; Paik, U. Arrays of Sealed Silicon Nanotubes as Anodes for Lithium Ion Batteries. *Nano Lett.* **2010**, *10* (5), 1710–1716.

[62]   Park, M. H.; Kim, M. G.; Joo, J.; Kim, K.; Kim, J.; Ahn, S.; Cui, Y.; Cho, J. Silicon Nanotube Battery Anodes. *Nano Lett.* **2009**, *9* (11), 3844–3847.

[63] Yao, Y.; McDowell, M. T.; Ryu, I.; Wu, H.; Liu, N.; Hu, L.; Nix, W. D.; Cui, Y. Interconnected Silicon Hollow Nanospheres for Lithium-Ion Battery Anodes with Long Cycle Life. *Nano Lett.* **2011**, *11* (7), 2949–2954.

[64] Ma, H.; Cheng, F.; Chen, J.-Y.; Zhao, J.-Z.; Li, C.-S.; Tao, Z.-L.; Liang, J. Nest-like Silicon Nanospheres for High-Capacity Lithium Storage. *Adv. Mater.* **2007**, *19* (22), 4067–4070.

[65] Liang, B.; Liu, Y.; Xu, Y. Silicon-Based Materials as High Capacity Anodes for next Generation Lithium Ion Batteries. *J. Power Sources* **2014**, *267*, 469–490.

[66] Liu, W.-R.; Wang, J.-H.; Wu, H.-C.; Shieh, D.-T.; Yang, M.-H.; Wu, N.-L. Electrochemical Characterizations on Si and C-Coated Si Particle Electrodes for Lithium-Ion Batteries. *J. Electrochem. Soc.* **2005**, *152* (9), A1719.

[67] Yu, H.; Liu, X.; Chen, Y.; Liu, H. Carbon-Coated Si/graphite Composites with Combined Electrochemical Properties for High-Energy-Density Lithium-Ion Batteries. *Ionics (Kiel).* **2016**, *22* (10), 1847–1853.

[68] Kim, H.; Seo, M.; Park, M. H.; Cho, J. A Critical Size of Silicon Nano-Anodes for Lithium Rechargeable Batteries. *Angew. Chemie - Int. Ed.* **2010**, *49* (12), 2146–2149.

[69] Zhu, S.; Zhu, C.; Ma, J.; Meng, Q.; Guo, Z.; Yu, Z.; Lu, T.; Li, Y.; Zhang, D.; Lau, W. M.; Abernathy, H. W.; Summers, C. J.; Liu, M. L.; Sandhage, K. H. Controlled Fabrication of Si Nanoparticles on Graphene Sheets for Li-Ion Batteries. *RSC Adv.* **2013**, *3* (17), 6141.

[70] Agyeman, D. A.; Song, K.; Lee, G. H.; Park, M.; Kang, Y. M. Carbon-Coated Si Nanoparticles Anchored between Reduced Graphene Oxides as an Extremely Reversible Anode Material for High Energy-Density Li-Ion Battery. *Adv. Energy Mater.* **2016**, *6* (20), 1–10.

[71]   Guo, Z. P.; Wang, J. Z.; Liu, H. K.; Dou, S. X. Study of Silicon/polypyrrole Composite as Anode Materials for Li-Ion Batteries. *J. Power Sources* **2005**, *146* (1), 448–451.

[72]   Chew, S. Y.; Guo, Z. P.; Wang, J. Z.; Chen, J.; Munroe, P.; Ng, S. H.; Zhao, L.; Liu, H. K. *Novel Nano-Silicon/polypyrrole Composites for Lithium Storage*; 2007; Vol. 9.

[73]   Du, Z.; Zhang, S.; Liu, Y.; Zhao, J.; Lin, R.; Jiang, T.; Weng, D.; Cui, Y.; Mahurin, S. M.; Besmann, T. M.; Dai, S. Facile Fabrication of Reticular Polypyrrole–silicon Core–shell Nanofibers for High Performance Lithium Storage. *J. Mater. Chem.* **2012**, *22* (23), 11636.

[74]   Botas, C.; Carriazo, D.; Zhang, W.; Rojo, T.; Singh, G. Silicon-Reduced Graphene Oxide Self-Standing Composites Suitable as Binder-Free Anodes for Lithium-Ion Batteries. *ACS Appl. Mater. Interfaces* **2016**, *8* (42), 28800–28808.

[75]   Ruffo, R.; Hong, S. S.; Chan, C. K.; Huggins, R. A.; Cui, Y. Impedance Analysis of Silicon Nanowire Lithium Ion Battery Anodes. *J. Phys. Chem. C* **2009**, *113* (26), 11390–11398.

[76]   Jana, M.; Sil, A.; Ray, S. Morphology of Carbon Nanostructures and Their Electrochemical Performance for Lithium Ion Battery. *J. Phys. Chem. Solids* **2014**, *75* (1), 60–67.

VITA

Tianxiang Ning

Candidate for the Degree of

Master of Science

Thesis: DESIGNING SILICON BASED ANODE FOR LITHIUM-ION BATTERIES

Major Field: Materials Science and Engineering

Biographical:

Education:

Completed the requirements for the Master of Science in Materials Science and Engineering at Oklahoma State University, Stillwater, Oklahoma in May, 2017.

Completed the requirements for the Bachelor of Engineering in Materials Science and Engineering at Hunan University, Changsha, Hunan in 2014.

Experience:
Graduate Research Assistant under Dr. Raj. Singh from 2015-2017.